2021

Cosmological gravitational waves: Refining a general rule of thumb for reheating

David Zhou
Bowdoin College

Cosmological gravitational waves: Refining a general rule of thumb for reheating

An Honors Paper for the Department of Physics and Astronomy

By David Zhou

Bowdoin College, 2021

Abstract

There are predictions for cosmological gravitational wave backgrounds from reheating based on various models. But, these predictions do not address the question of how an observed spectrum relates back to an unknown model or parameter. Given this problem, we have numerically and analytically investigated a variety of chaotic inflation models and their gravitational wave spectra.

We studied chaotic inflation potentials $V(\phi) = \lambda f(\phi/\phi_0) + \frac{1}{2}g^2\phi^2\chi^2$. λ determines the curvature of the potential and g^2 quantifies how strongly fields ϕ and χ are coupled to each other. For these chaotic inflation potentials, we found the peak frequency to be proportional to the parameter $\lambda^{1/4}$. So, given an observed peak frequency, we can identify which model that peak frequency must correspond to.

We also found a two-class amplitude behavior for otherwise close values of the coupling parameter g^2/λ. In exploring this puzzle, we found that this behavior emerges directly from the exponential pre-heating phase after inflation as a result of different exponential growth rates.

To refine our understanding of amplitude, we investigated the β, which describes how quadrupolar the gravitational wave source's energy density is. We found reasonable agreement between our analytic estimate and other existing estimates for β, indicating that we captured a good amount of the relevant physics. But to learn more about β, we need to study how initial fluctuations in the field sourcing gravitational waves χ grow and contribute to the source's stress energy tensor.

Contents

Chapter 1

Introduction

Our initial understanding of the Big Bang came with some puzzles. Why are apparently causally unrelated points in our Universe measured to have a temperature of 3 K? Why are the Universe's energy density parameters so finely tuned to give us a flat Universe? Where are all the early universe magnetic monopoles and why haven't we found any? Alan Guth and Andrei Linde proposed a resolution to these puzzles: inflation. They argued that the early Universe expanded by a factor of about 60 e-folds between $t = 10^{-36}$ s to $t = 10^{-33}$ s [1] [2].

Since inflation was proposed, cosmologists have developed a variety of scalar field models to describe inflation. For now, we only have a limited way of evaluating which models properly describe inflation and which ones don't. First, we have no observational evidence of inflation (for now). Second, even if we had observational evidence of inflation, we wouldn't have any analytic relations to compare a direct observation with underlying models.

So what can we do? We currently don't have the tools to address the first problem. But, we do have all the tools to address the second problem. There are plenty of models to work with, excellent numerical simulations that predict observations given a particular model, and existing analytic work that we can build on.

With these tools in hand and some underlying knowledge of gravitational wave production and cosmology, we wish to find analytic relationships between inflation models and their parameters with future observables or gravitational wave features. We use numerical simulations as guardrails to test and compare our analytic investigation's assumptions and results.

There is already literature making analytic predictions for gravitational waves from cosmological sources. In particular, Dufaux et al. connect gravitational wave energy density to an inflaton field modelled as a wave packet [3] given a chaotic potential. Giblin and Thrane produce a 'rough rule of thumb' for what gravitational waves look like from a generic cosmological source (meaning they do not make any model constraints on what the source's stress energy tensor T_{ij} looks like) [4].

We wish to expand on Dufaux and Giblin and Thrane's work by analytically investigating gravitational wave energy density for more than one inflation model and seeing how those model constraints can tell us about the source of gravitational waves, and therefore gravitational wave energy density.

We organize the discussion and analysis as follows. The remainder of this chapter introduces how expansion is described in cosmology, how inflation is described within that context, and how our cosmological gravitational waves are different from astrophysical gravitational waves. Chapter 2 introduces the existing work that we are going to use and build off. Chapter 3 is a compilation of numerical results from simulating reheating and producing gravitational waves from Zhiqi Huang's numerical simulation HLattice [12]. Chapter 4 details the analytic investigation we undertook to understand the underlying physics of one of our numerical results for gravitational wave peak frequency. Chapter 5 provides a more detailed investigation into the underlying physics associated with gravitational wave amplitude. In chapter 6, we discuss the implications of our results and possibilities for further investigation.

1.1 Background

1.1.1 How cosmologists describe expansion

Inflation is ultimately a description of early Universe expansion. So we want to introduce how cosmologists describe expansion.

In 1929, Edwin Hubble observed that the further a particular galaxy was from Earth, the faster it travelled away from us [6]. More specifically, he observed

$$v = Hr \tag{1.1}$$

where v and r are speed and distance. Eqn (1.1) is Hubble's law. The proportionality parameter H is most commonly quoted in units of km/s/Mpc. Today, this parameter is measured to be approximately $H_0 = 70$ km/s/Mpc.

We need a useful way to compare distances across large scale structures at different points in time in an expanding Universe. To do this, we can describe physical distances in our Universe using a dimensionless 'scale factor' $a(t)$. If $a(t_1) = 3$ and $a(t_0) = 1$, then

$$r(t_1) = 3r(t_0) \tag{1.2}$$

where the convention is to choose $a = 1$ for today. We can combine this relation between scale factor and distances, Eqn (1.2), with Hubble's Law, Eqn (1.1), to show that

$$H = \frac{\dot{a}}{a}. \tag{1.3}$$

We now have two quantities that describe our Universe's expansion: a and H. In more colloquial terms, the scale factor a can be used to compare how much 'bigger' or 'smaller' the Universe is as a result of expansion between two points in time. The Hubble parameter H can be thought of as how quickly scale factor a is growing.

Next, we want to model a and H. To do describe the dynamics of a and H, Alexander Friedmann combined the assumption of a spatially homogeneous and isotropic Universe with Einstein's field equations. The 00 component of Einstein's field equations gives "Friedmann's first equation:"

$$\dot{a} = H_0 \left(\frac{\Omega_{m,0}}{a} + \frac{\Omega_{r,0}}{a^2} + a^2 \Omega_{\Lambda,0} \right)^{1/2}. \tag{1.4}$$

Here, $\Omega_{m,0}$, $\Omega_{r,0}$, and $\Omega_{\Lambda,0}$ are unitless parameters that compare the today's values for density of matter, radiation, and cosmological constant in the Universe to the critical density today. They are defined as

$$\Omega_i \equiv \frac{\rho_i}{\rho_{critical}} \tag{1.5}$$

where $\rho_{critical}$ is the critical density, or the specific matter density needed to have a spatially flat Universe. Eqn (1.4) tells us how our scale factor a evolves over time in response to different matter densities.

Another useful equation that helps us describe scale factor a is the Friedmann acceleration equation

$$\frac{\ddot{a}}{a} = -\frac{4\pi G}{3} \left(\rho + \frac{3P}{c^2} \right) \tag{1.6}$$

where ρ is matter density and P is pressure. For convenience, we choose units where $c = 1$ and $G = 1$ for Eqn (1.6) and get

$$\frac{\ddot{a}}{a} = -\frac{4\pi}{3}(\rho + 3P). \tag{1.7}$$

This acceleration equation is useful because we can combine it with an equation of state to relate pressure P and density ρ. Doing so leaves us with scale factor as an ordinary differential equation as a function of matter density ρ.

On large scales, we describe the Universe using the perfect fluid equation of state:

$$P = w\rho, \tag{1.8}$$

where w is the equation of state parameter. So Eqn (1.6) can then be written as

$$\frac{\ddot{a}}{a} = -\frac{4\pi}{3}(1+3w)\rho. \tag{1.9}$$

In general, ρ is a function of a. We can further constrain ρ by using conservation of mass-energy to find

$$\dot{\rho} = 3H(\rho + P), \tag{1.10}$$

which is solved by

$$\rho = \rho_0 a^{-3(1+w)}. \tag{1.11}$$

For a radiation dominated universe, $w = 1/3$, and $\rho \propto a^{-4}$. For a matter dominated universe, $w = 0$, and $\rho \propto a^{-3}$. However, if we let $w = -1$, $\rho = \rho_0$ (i.e, the density is constant). If this density term is constant, Eqn (1.6) is simplified so that

$$a(t) \propto \exp\left[\frac{8\pi}{3}\rho_0 t\right]. \tag{1.12}$$

The takeaway here is that we get exponential expansion when we let our equation of state parameter $w = -1$.

1.1.2 Inflation dynamics

Now we want to learn how inflation is modelled and how inflation gives us $w = -1$. Inflation is described by the 'inflaton' field ϕ. This scalar field ϕ can be thought of as having a scalar value for every point in space where particle behaviors are just excitations in that field, like how photons can be thought of as excitations in the electromagnetic

field.

The inflaton field has energy (and energy density) associated with it. Its stress-energy tensor is

$$T^{\mu}_{\ \nu} = (\partial^{\mu}\phi)(\partial_{\nu}\phi) - \delta^{\mu}_{\ \nu}\mathcal{L} \tag{1.13}$$

where

$$\mathcal{L} = \frac{1}{2}(\partial_{\mu}\phi)^2 - V(\phi) \tag{1.14}$$

with the following equation of motion:

$$\ddot{\phi} + 3H\dot{\phi} + \frac{dV}{d\phi} = 0. \tag{1.15}$$

Here, the Lagrangian density $\mathcal{L}$ is related to the more familiar Lagrangian L

$$S = \int dt L(x, \dot{x}) \tag{1.16}$$

where S denotes the action. The Lagrangian density is then defined such that

$$L = \int d^3x \mathcal{L}. \tag{1.17}$$

This quantity is popular in field theory because the action principle for a single field ϕ is defined a bit differently from how the action is denoted in nonrelativistic mechanics:

$$\mathcal{S} = \int d^4x \mathcal{L}(\phi, \dot{\phi}) \tag{1.18}$$

We can write the stress-energy tensor as that of a perfect fluid,

$$T^{\mu}_{\nu} = \begin{pmatrix} \rho & 0 & 0 & 0 \\ 0 & -P & 0 & 0 \\ 0 & 0 & -P & 0 \\ 0 & 0 & 0 & -P \end{pmatrix}, \tag{1.19}$$

if we identify

$$\begin{aligned} \rho &= \frac{1}{2}\dot{\phi}^2 + V(\phi) \\ p &= \frac{1}{2}\dot{\phi}^2 - V(\phi). \end{aligned} \tag{1.20}$$

Now combining the above for ρ and P with the perfect fluid equation of state Eqn. (1.8) gives us [13]:

$$w \equiv \frac{P}{\rho} = \frac{\frac{1}{2}\dot{\phi}^2 - V(\phi)}{\frac{1}{2}\dot{\phi}^2 + V(\phi)}. \tag{1.21}$$

Notice that if the kinetic term $\dot{\phi}$ is small and the potential term $V(\phi)$ is large (and so is ϕ), we have

$$w \approx -\frac{V}{V} = -1. \tag{1.22}$$

With $w = -1$, we get exponential expansion. Once $w \neq -1$, inflation ends and we recover the expansion history that we are familiar with. Cosmologists further quantify this state of low kinetic energy and high potential with the slow-roll parameters

$$\epsilon(\phi) = \frac{M_p^2}{2}\left(\frac{V'}{V}\right) \tag{1.23}$$

and

$$\eta(\phi) \equiv M_p^2 \frac{V''}{V} \tag{1.24}$$

where $V' = dV/d\phi$ and $V'' = d^2V/d\phi^2$. Inflation ends when these slow roll parameters $\eta = \epsilon = 1$.

1.1.3 Reheating

There is one problem from our introduction that requires more explanation. We like inflation because it 'inflates' many of the Big Bang's problems away, including the magnetic monopoles problem. But if inflation lowers the density of early magnetic monopoles away, it should also do the same for all the other forms of matter we know and love. Why is there anything? This answer lies in a process called reheating. Once inflation ends, inflaton field decays into the Standard Model particles we know and love. This period after inflation is called reheating.

If we look at our inflaton's equation of motion Eqn (1.15), we'll notice that it acts as an oscillator. That said, the does not behave as a simple harmonic oscillator, but an anharmonic oscillator, which means that the inflaton's restoring force will not be proportional to amplitude. This means that the inflaton's oscillation period can depend on its amplitude. What is our inflaton field oscillating about? Most inflaton potentials have some shape shown in Fig. 1.1.

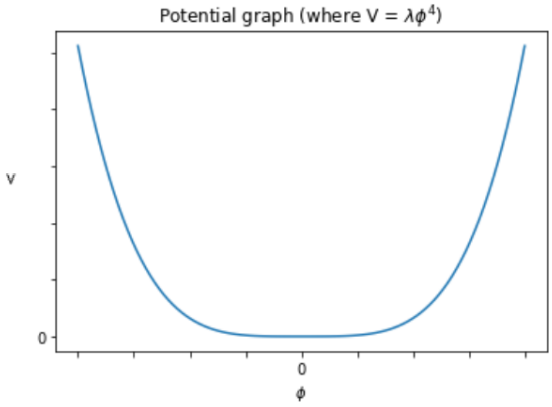

(a)

Figure 1.1: Inflaton potential given a specific potential model $V = \lambda\phi^4$.

Our inflaton field wants to approach its lowest energy state at the bottom of the potential. While on the sides of the potential graph, the field value is big. Inflation occurs when the field value is big. After inflation, the inflaton field ϕ will have a small value and oscillate about the bottom of the potential until the inflaton finally comes to

a rest. While the inflaton is oscillating about the bottom, we have 'reheating.'

We have to be careful about how we analyze ϕ during reheating. We have talked about our inflaton field ϕ in the context of Eqn (1.15), which only depends on time. Eqn (1.15) assumes the inflaton field to be spatially homogeneous. At a more detailed level, the inflaton field has a homogeneous part and spatially dependent perturbations. This more detailed description can be expressed as $\phi(t, \mathbf{x}) = \phi_{homogeneous}(t) + \delta\phi(\mathbf{x})$ where $\delta\phi$ represents the small perturbations. For large values of ϕ, ϕ is approximately $\phi_{homogeneous}$. The small perturbations are negligible. Once the inflaton field value gets smaller and oscillates about its zero value, these small perturbations become a larger proportion to the overall size of ϕ and thus become important when calculating the inflaton field's value.

It is helpful to think of this like measuring depths of two different bodies of water: an ocean and a wave pool. The height of these bodies of water can be thought of as the field value ϕ we're interested in and the waves atop can be thought of as the perturbations. All other water is then analogous to the homogeneous part.

When measuring the depth of the ocean, you aren't going to worry about the relatively small wave heights on the surface. But when measuring the depth of a wave pool at a particular location in the pool, the size of the wave will play a significant role in an accurate measurement of pool depth.

During reheating, $\phi_{homogeneous}$ is much smaller than it was during inflation, meaning we have to account for small perturbations $\delta\phi$. It is no longer appropriate to allow ϕ to only obey its one-dimensional equation of motion Eqn (1.15). Accounting for these spatially dependent perturbations is why numerical simulations are important for modelling inflaton behavior.

The field actually responsible for reheating is a hypothetical matter producing field χ. If we allow our inflaton field to couple to χ, then as our inflaton field is oscillating about the bottom of its potential graph, it acts as χ's driving force. In other words, the

inflaton field ϕ and our matter-producing field χ can be thought of as a driving force and driven oscillator respectively. In such a system, the driven oscillator responds better and produces stronger oscillations at certain frequencies and responds poorer and produces weaker oscillations at other frequencies. The frequencies where the driven oscillator produces stronger oscillations are resonant frequencies.

We are focused on parametric resonance. Parametric resonance is the phenomenon where, an oscillator's amplitude will grow exponentially at particular resonant frequencies. When χ achieves parametric resonance during reheating, χ's matter production continues to get amplified until the end of reheating, giving us a lumpy distribution of matter.

As our inflaton oscillates at the bottom of its potential graph at different frequencies, it'll drive this χ field at different frequencies. This χ field oscillating at different frequencies will produce an uneven distribution of matter. Where there's an uneven distribution of matter, we get gravitational waves.

So, reheating is the phenomenon that gives back the matter that would otherwise have been inflated away. It is through gravitational waves from reheating that we can get observations and insight into inflation. The details to this can be found in Section 2.1.2.

1.1.4 Gravitational waves from cosmological sources

Gravitational waves are small perturbations in the curvature of spacetime created by inhomogeneities in the distribution of matter and energy. But, there is a difference between cosmological gravitational waves and the more famous gravitational waves from the past couple of years.

Signals from an acute astrophysical event that happened in one particular place in space, like a black hole merger, have been observed. We are interested in potential observations of signals from 'reheating,' the process where inflaton coupling produces a

'lumpy' distribution of matter/energy in our early Universe.

There is also a more technical difference to note. The frequencies LIGO is sensitive to are on the order of tens to hundreds of hertz (Hz). The cosmological signals that we are interested in are on the order of 10^7 to 10^9 Hz. So we are looking for frequencies many millions of times larger than what we have the equipment to observe for the time being. But, there are no current or planned experiments looking for these signals.

Current and planned gravitational wave experiments like LISA or Advanced LIGO won't be particularly sensitive to these frequencies. They are sensitive around frequencies on the order of Hz and can measure amplitudes of 10^{-5} to maybe 10^{-14} [9]. But, there are proposals like DECIGO and B-DECIGO that are aimed at looking for early Universe background gravitational waves specifically [10].

This motivates us to learn more about gravitational wave production from the inflaton field. Giblin and Thrane have given us a good general starting point for these cosmological gravitational waves from a generic source [4]. Dufaux et al have given us a very useful way to relate inflation potential parameters of one particular model to the gravitational wave energy density [3]. What we want to do is think about what generalities exist across models. We want to use those cross-model generalities to tell us about gravitational wave signal predictions across models, rather than signals related to only one model. Doing so will allow us to look at a spectrum one day and identify which model accurately describes inflation.

Chapter 2

Existing Literature and Methods

Giblin and Thrane derive a 'rule of thumb' relation between gravitational wave signals and some generic cosmological source [4]. Dufaux et al make analytic predictions for gravitational waves from a particular inflation potential [3]. We can use Dufaux's result for what this source ought to look like for a variety of different inflation potentials. Given a source for a variety of models, we can look at what gravitational wave signals ought to look like from a variety of different inflation parameters and potentials.

2.1 Existing literature

2.1.1 A rule of thumb for cosmological gravitational waves

Giblin and Thrane derive what they call a 'rule of thumb' relation between gravitational wave signals and a generic cosmological source. They do this by assuming some generic source that is Gaussian distributed in momentum space (or 'k-space') about some characteristic scale k_*

$$\tilde{T_{ij}}(\mathbf{k}) = A_{ij} \exp\left[-\frac{(|\mathbf{k}| - k_*)^2}{2\sigma^2}\right] \tag{2.1}$$

where $\tilde{T_{ij}}$ denotes the Fourier transform of T_{ij}, A_{ij} is the peak height and is generally complex, and σ parameterizes the source width. To constrain the amplitude A_{ij}, Giblin

and Thrane want to find a way to represent it in terms of the gravitational wave source's energy density ρ_s (which can be represented as a fraction of the total energy density of the Universe).

If the source can be described by an isotropic pressure p_s and as a perfect fluid, it obeys

$$\tilde{\rho}_s(\mathbf{k}) = \frac{\tilde{p}_s(\mathbf{k})}{w} = \frac{\tilde{T}(\mathbf{k})}{w} \tag{2.2}$$

where w is the equation of state parameter. They then assume a large enough volume so that the energy density is homogeneous. They then invoke Parseval's theorem

$$\int d^3k |\tilde{\rho}_s(\mathbf{k})|^2 = \int dV \rho_s^2(\mathbf{x}) = V\rho_s^2. \tag{2.3}$$

Therefore,

$$V\rho_s^2 = \int d^3k |\tilde{\rho}_s(\mathbf{k})|^2 = \int d^3k \frac{|\tilde{T}_s(\mathbf{k})|^2}{w^2}. \tag{2.4}$$

This is then combined with Eqn (2.1) to show that

$$|A|^2 = \frac{w^2\rho_s^2 V}{W} \tag{2.5}$$

where

$$W \equiv 4\pi \int k^2 \exp\left[\frac{-(k-k_*)^2}{\sigma^2}\right] dk. \tag{2.6}$$

The source energy density ρ_s is a fraction of the total energy density of the Universe ρ, i.e $\rho_s = \alpha\rho$ where $\alpha < 1$, leaving us with

$$|\tilde{T}|^2 = \frac{w^2\alpha^2 V\rho^2}{W} \exp\left[-\frac{-(k-k_*)^2}{\sigma^2}\right]. \tag{2.7}$$

Here, the source's stress energy tensor $\tilde{T}$ loses its directional dependence because Giblin and Thrane assume the source to be isotropic.

This representation of the source energy is important because metric perturbations

obey

$$\ddot{h}_{ij} + 3H\dot{h}_{ij} - \frac{1}{a^2}\nabla^2 h_{ij} = 16\pi T^{TT} \tag{2.8}$$

where we have the transverse-traceless projection of the source's stress energy tensor

$$T^{TT}_{ij} = T_{ij} - \frac{\delta_{ij}}{3}T^k_k. \tag{2.9}$$

This sourced Klein-Gordon equation is made simpler by assuming the source to be short-lived compared to Hubble-time, meaning we can neglect the friction term. When h takes a maximum the acceleration term disappears, leaving

$$\tilde{h} \approx \tilde{h}_{ij} \approx \frac{16\pi}{k^2}T^{TT}. \tag{2.10}$$

They then define a new parameter

$$\beta \equiv \frac{|T^{TT}|^2}{|T|^2}. \tag{2.11}$$

Then they use

$$\Omega_{gw}(k) = \frac{k^3}{32\pi\rho V}\sum_{i,j}\int d\Omega |\dot{h}^{TT}_{ij}|^2 \tag{2.12}$$

where

$$|\dot{h}|^2 = |h|^2k^2 = (16\pi G)^2\frac{\beta|\tilde{T}|^2}{k^2} \tag{2.13}$$

and Ω_{gw} is the gravitational wave energy density [11]. They then combine Eqn (2.13) and Eqn (2.12) with the Friedmann equation to show

$$\Omega_{gw}(k_*) \approx 108\pi\alpha^2\beta w^2 N \tag{2.14}$$

where

$$N \equiv \frac{H^2k_*}{W}. \tag{2.15}$$

This is then redshifted to today and evaluated to

$$\Omega_{gw,0}(k_*) \approx 4.7 \times 10^{-8} \alpha^2 \beta w^2. \tag{2.16}$$

This result is what Giblin and Thrane call a 'rule of thumb' estimate for cosmological gravitational waves. Here, α is the fraction of the Universe's energy density that contributes to the source's energy density, β describes how quadrupolar the source energy density is or how much of the source's energy goes towards gravitational wave production, and w is the source's equation of state parameter.

Giblin and Thrane assume that the source is Gaussian distributed in k-space about a mean frequency k_*. They also assume that the source's stress energy tensor has a complex amplitude factor A_{ij}. They let β be described by a random process and estimate it numerically. They assume each component A_{ij} to be A multiplied by a different random complex phase factor.

They leave open what underlying models might might actually describe β and A_{ij}. What we want to do is impose a physical model on β, estimate gravitational waves from our calculation of β, and learn about how β depends on inflation parameters and potentials.

More specifically, we choose χ to be our source for gravitational waves and β, where χ is going to depend on how we describe ϕ. We describe ϕ as an oscillating scalar field, which means that

$$T^{\mu}_{\ \nu} = \partial^{\mu}\phi\partial_{\nu}\phi - \delta^{\mu}_{\ \nu}\mathcal{L} \tag{2.17}$$

where

$$\mathcal{L} = \frac{1}{2}(\partial_{\mu}\phi)^2 - V(\phi). \tag{2.18}$$

We want to look for generalities in the inflaton's behavior that exist across different potentials, relate inflaton behavior to gravitational wave signals, and learn how those signals relate back to what we learned about V.

Dufaux et al compute gravitational wave energy density from a particular inflation model. If we want to calculate gravitational wave energy density across different models, it will be useful to first understand how to do it for one model.

2.1.2 Gravitational waves given a particular inflation model

We have predictions about what gravitational waves might look like for a generic cosmological source [4]. What we want to do now is think about what this source ought to look like given a scalar field model.

We can represent the transverse-traceless stress energy tensor from some homogeneous scalar field η in momentum-space or k-space as:

$$T_{ij}^{TT}(\mathbf{k}) = \mathcal{O}_{ij,lm}(\mathbf{k}) \int \frac{d^3\mathbf{p}}{(2\pi)^{3/2}} p_l p_m \eta(\mathbf{p}) \eta(\mathbf{k}-\mathbf{p}) \tag{2.19}$$

where $\mathbf{p}$ is the field momentum, and $\mathcal{O}_{ij,lm}$ is the transverse-traceless projection operator defined as

$$\mathcal{O}_{ij,lm}(\mathbf{k}) \equiv \left[P_{il}P_{jm} - \frac{1}{2}P_{ij}P_{lm} \right] \tag{2.20}$$

where

$$P_{ij} = \delta_{ij} - \hat{k}_i \hat{k}_j. \tag{2.21}$$

We can further describe this scalar field source by ascribing a particular potential to it. Dufaux et al consider the following potential [3]

$$V = \frac{1}{4}\lambda\phi^4 + \frac{1}{2}g^2\phi^2\chi^2 \tag{2.22}$$

where λ determines how flat or sharp the potential curve is and g^2 is the coupling parameter describing how strongly ϕ is coupled to χ.

Here, our potential is stated in units where $G = \hbar = c = 1$. Our parameters λ and g^2 are dimensionless. However, it will be useful to explicitly state the first term on

the right hand side of our potential in dimensionful quantities. Doing so will allow us to use that first term to make dimensionful predictions in a later section.

We start with the action principle, which has units of energy $\times$ time:

$$\mathcal{S} = \int d^4x \mathcal{L}. \tag{2.23}$$

where

$$\mathcal{L} = \frac{1}{2}\dot{\phi}^2 - (\nabla\phi)^2 - V(\phi). \tag{2.24}$$

By recognizing that both sides of the Eqn (2.23) must have units of energy $\times$ time, we can find that the units of $\mathcal{L}$ must be

$$\frac{\text{energy} \times \text{time}}{\text{length}^4}. \tag{2.25}$$

Therefore, the gradient term for ϕ in Eqn (2.24) must also have the same units of $\mathcal{L}$. The numerical simulation we use quotes ϕ in units of Planck mass M_p. With this information about ϕ and units of $\mathcal{L}$, we can find that ϕ must be multiplied by a factor of $c/\hbar^{1/2}$.

Eqn (2.24) also requires that $V(\phi)$ have the same units as $\mathcal{L}$. We know that ϕ^4 multiplied by $c^4/\hbar^2$ has units of

$$\frac{(\text{energy} \times \text{time})^2}{\text{length}^4}. \tag{2.26}$$

With the units of $\phi^4 c^4/\hbar^2$, we finally match units of V and $\mathcal{L}$ by dividing λ by a factor of $\hbar$. So in dimensionful quantities and neglecting the second term, Eqn (2.22) becomes

$$V = \frac{\lambda c^4}{4\hbar^3}\phi^4. \tag{2.27}$$

Now that we understand the potential associated with our scalar field source, we have to be careful about which scalar field sources gravitational waves. We should not

expect gravitational waves from ϕ, but χ.

Recall from Section 1.1.3, certain frequency modes of χ being amplified more than others. As a result, χ will have a less uniform spatial energy distribution. These anisotropies in χ's energy distribution grow with parametric resonance and are ultimately what sources gravitational waves. So because χ sources gravitational waves, we compute Eqn (2.19) with χ, not ϕ.

Now Dufaux et al need a functional form for χ to use with Eqn (2.19). Recall that the χ field behaves as a driven oscillator where the inflaton ϕ acts as its driving force. Dufaux et al solve for a rescaled χ from

$$\frac{d^2 X_k}{dx^2} + \omega_k^2(x) X_k = 0 \tag{2.28}$$

where

$$\omega_k^2(x) = K^2 + q\bar{f}^2(x) \tag{2.29}$$

and

$$X_k = a\chi \text{ for some choice of } k,\ K = \frac{k}{\sqrt{\lambda}\phi_0},\ q = \frac{g^2}{\lambda},\ \bar{f} = \frac{a\phi}{\phi_0} \tag{2.30}$$

Dufaux et al use X_k and solve for the spectrum using complicated elliptic integrals among other things. We will not dive deeply into the result or how they got it. But, the process of solving for the inflaton field ϕ, using ϕ to describe χ's frequency, and solving for χ which will ultimately give us the source's stress energy tensor is what we are particularly focused on.

We undertake a similar investigation for different inflaton potential models. Different inflaton potential models give different inflaton fields, as we can see in Eqn. (1.15). Different ϕ values means a different driving force for χ. A different χ means a different stress energy tensor sourcing gravitational waves, which means a different spectrum. We hope to do this calculation from ϕ to the gravitational wave spectrum. In doing so, we hope to capture the relevant physics involved with gravitational wave production from

reheating.

We will not be solving for ϕ analytically. We are going to use numerical solutions for different fields ϕ to simplify our calculations.

2.2 Numerical simulation

It is useful to have a numerical simulation on hand to guide and compare our analytic investigation. Because we are studying an exponentially growing source χ, any approximations we make may be unreliable without the support from a full simulation. Furthermore, having a numerical simulation ensures that we don't stray down any wrong paths, and can give us assumptions that we can use to simplify our analytic investigation.

For example, before diving into any analytic investigation, we can first numerically test how gravitational wave amplitudes might vary with some parameter λ from some potential $V = \lambda\phi^4$. The numerical results might show that gravitational wave amplitudes are independent of or very weakly dependent on λ. That numerical conclusion will save us the time of finding the same result analytically.

We will simulate gravitational waves using Zhiqi Huang's HLattice simulation [12]. During inflation, the inflaton field ϕ is approximately homogeneous. The inflaton field has small perturbations that are ultimately important during reheating, but are not consequential during inflation.

Because of the inflaton field's homogeneity during inflation, HLattice first solves for ϕ from its equation of motion Eqn (4.1) and the Friedmann equation Eqn (1.4). This numerical integration ends when the condition Eqn (1.22) is no longer true. More specifically, the simulation runs until the kinetic term is no longer small, or

$$-\frac{\dot{\phi}}{\phi} > H. \tag{2.31}$$

To calculate ϕ during reheating, the inflaton field is represented as a lattice where

every point on the lattice is initialized with some small perturbation. Small perturbations at each point will give a different field value.

Given a different field value, ϕ will have a different Hamiltonian, which will tell us about the distribution of energy in momentum space. That distribution is going to be anisotropic. And from anisotropic distributions of energy comes gravitational waves.

These gravitational waves are then calculated from the anisotropic energy distribution. Then there is a time step where the perturbations obey Hamilton's equations. These new perturbations give us a new field value. The simulation continues to do this until some chosen maximum scale factor is reached.

2.3 Choice of models

We saw Dufaux et al give us an expression for the gravitational wave spectrum for a specific inflaton potential Eqn (2.22). We ultimately want to see what this spectrum looks like across different inflaton potentials. The specific potentials we investigate are the same inflaton potentials explored in Hooper's work [5].

$$V = \lambda\phi_0^4 f\left(\phi/\phi_0\right) + \frac{1}{2}g^2\phi^2\chi^2 \tag{2.32}$$

where we define

$$\psi \equiv \frac{\phi}{\phi_0} \tag{2.33}$$

and

$$f(\psi) = \begin{cases} \psi^4 \equiv \text{Model 1 potential} \\ \arctan^4 \psi \equiv \text{Model 2 potential} \\ \tanh^4 \psi \equiv \text{Model 3 potential} \\ \left[1 - \exp\left(-\psi^2\right)\right]^2 \equiv \text{Model 4 potential} \\ \left(1 - \cos\psi\right)^2 \equiv \text{Model 5 potential} \\ \psi^4/(1+\psi^2)^2 \equiv \text{Model 6 potential} \end{cases} . \tag{2.34}$$

Note that Eqn (2.32) is just a generalization of the potential from earlier Eqn (2.22).

We choose these particular models because they give an inflaton field solved by an attractor solution. Having a system described by an attractor solution means that a system tends to evolve towards a narrow set of states from a wide range of initial conditions. This can be seen by graphically representing the phase space of a chaotic inflaton, where the system will evolve along the trajectories which the slopes are tangent in Fig. 2.1.

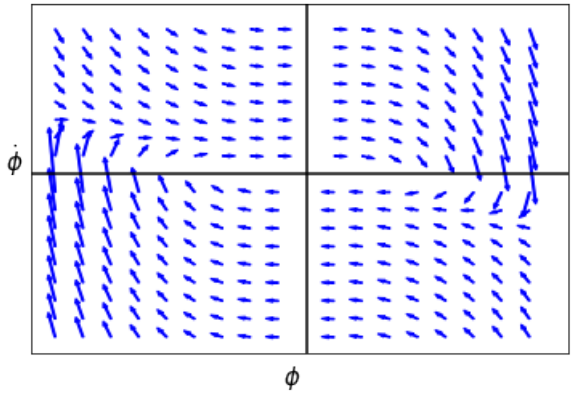

Figure 2.1: We have a variety of slopes plotted on the phase space between ϕ and $\dot{\phi}$. We can see that wherever you start takes the state towards the cyclone-like center. This is to say that for a variety of initial conditions, the system ultimately evolves towards the same state.

What we have plotted here is a variety of slopes for different values of ϕ and $\dot{\phi}$. This slope can be calculated from the equation of motion Eqn (1.15) and the Friedmann

equation (1.4):

$$\frac{d\dot{\phi}}{d\phi} = \frac{3\dot{\phi}\left(\frac{8\pi}{3}\left(\frac{1}{2}\dot{\phi}^2 + \frac{1}{2}\lambda\phi^4\right)\right)^{1/2}}{\dot{\phi}}. \tag{2.35}$$

The attractor solution means that these particular inflation models are less sensitive to initial conditions. We should not expect wildly different inflaton behavior (and thus gravitational wave signals) because of initial conditions that we don't know much about for now and can't test for.

It is important to note that chaotic inflation models are not the only types of inflation models. In other words, this project does not explore generality across all inflation models, rather a broad class of inflation models.

2.4 Goals of this work

We want the ability to point to specific features in gravitational wave spectra and identify what model and parameter must describe inflation. To get at that goal, we investigate gravitational wave spectra for different models and parameter values using HLattice. We do this investigation by running HLattice for each potential. For each potential, we let look at how gravitational wave frequency and amplitude vary for different inflation parameter values. We can then do a curve fit of the gravitational wave spectra with the parameter values.

We want to use our analytic investigations to learn about what underlying physics might give us our numerical results. In doing so, we will gain a better understanding of how gravitational waves are produced from reheating and how gravitational waves might tell us about inflation parameters.

We approach our analytic investigation with the goal of doing the simplest calculation or putting together the simplest model possible that captures the essence of the underlying physics.

To better understand the physics involved with frequency and the underlying

parameters, we explore the spectra's peak frequency for a model 1 potential. We assume the gravitational wave frequency to have approximately the same frequency as its driving force and look to compute the driving force ϕ's frequency. In this calculation for inflaton frequency, we assume ϕ to be homogeneous. Therefore it obeys its homogeneous equation of motion Eqn (1.15). We integrate that equation of motion and express ϕ's period in terms of our model 1 potential parameters. From the period, we can compute frequency.

To better understand the physics involved with amplitude and the underlying parameters, we investigate the quadrupolar parameter β from Giblin and Thrane's work. β is dependent on the source tensor, which depends on χ. We can compute χ using its equation of motion Eqn (2.28), which depends on ϕ. We compute ϕ using its homogeneous equation of motion. And ϕ depends on the source parameters λ and g^2. So, the source parameters tell us about ϕ. ϕ tells us about χ. χ tells us about the source's stress-energy tensor. The source's stress-energy tensor tells us about β. In going through this calculation, we hope to capture the first-order relevant physics involved in gravitational wave amplitude.

Chapter 3

Numerical Results

We are interested in distinguishing inflation models based off of gravitational wave features. To do so, we examine how gravitational wave frequency and amplitude change when we change the value of our inflaton field parameter λ and the coupling parameter g^2 for different models.

For each model, we are going to simulate gravitational waves using HLattice for different values of λ while fixing g^2/λ. Then we simulate gravitational waves again for different values of g^2/λ while fixing λ [12]. For each parameter, we are going try and identify the existing relation between that parameter and the resulting gravitational wave frequency and amplitude.

3.1 Results for λ

We start by simulating gravitational waves with the Model 1 potential given by Eqn (2.32). We run HLattice at a simulation resolution of 64 (meaning 64 points on our lattice on a side of a 3D cube), a box size of 8 (representing a Universe 8 times the size of the initial Hubble distance), and a maximum scale factor a of 130 (which we chose by evaluating when the gravitational wave signal stopped evolving).

We then run the simulation to give us gravitational waves, each curve or signal

for a different value of λ. We also fix the coupling parameter to $g^2/\lambda = 120$. The results are shown in Fig. 3.1.

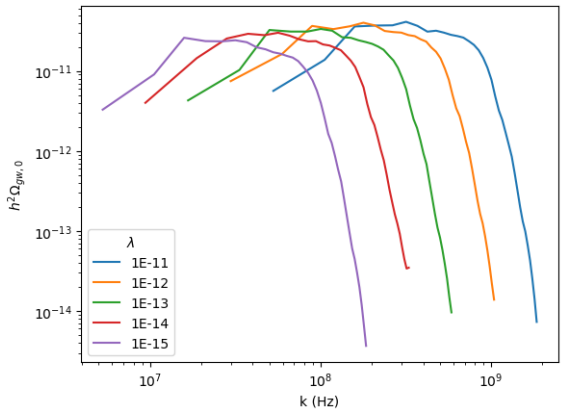

Figure 3.1: Gravitational wave signals in terms of frequency and amplitude for different λs given a model 1 potential. Each curve represents a gravitational wave signal with a different value of λ.

Fig. 3.1 shows that there is a positive relationship between λ and both amplitude and frequency. To find the specifics of this positive relation, we track the peak amplitude and see how this peak's amplitude and frequency change across curves or different values of λ. This is shown in Fig. 3.2.

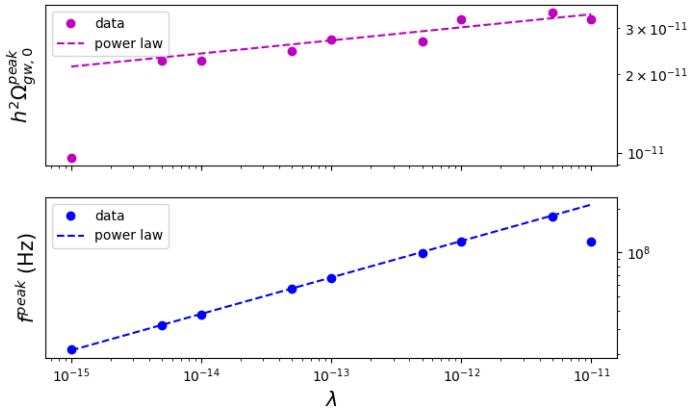

Figure 3.2: Each curve on Fig. 3.1 has a peak frequency, amplitude, and associated value of λ. Fig 3.2 tracks and plots the peak quantities with their associated values of λ.

Fig. 3.2 gives us a relationship between peak frequency f^{peak} and λ of

$$f^{peak} \approx (1.2 \times 10^{11})\ \lambda^{1/4}\ \text{Hz}. \tag{3.1}$$

Doing the same for the relationship between amplitude $h^2\Omega_{gw,0}$ and λ, we find

$$h^2\Omega_{gw,0}^{peak} \approx (1.5 \times 10^{-10})\ \lambda^{1/20}. \tag{3.2}$$

We can do this again for the other potential models for the results shown in Figure 3.3.

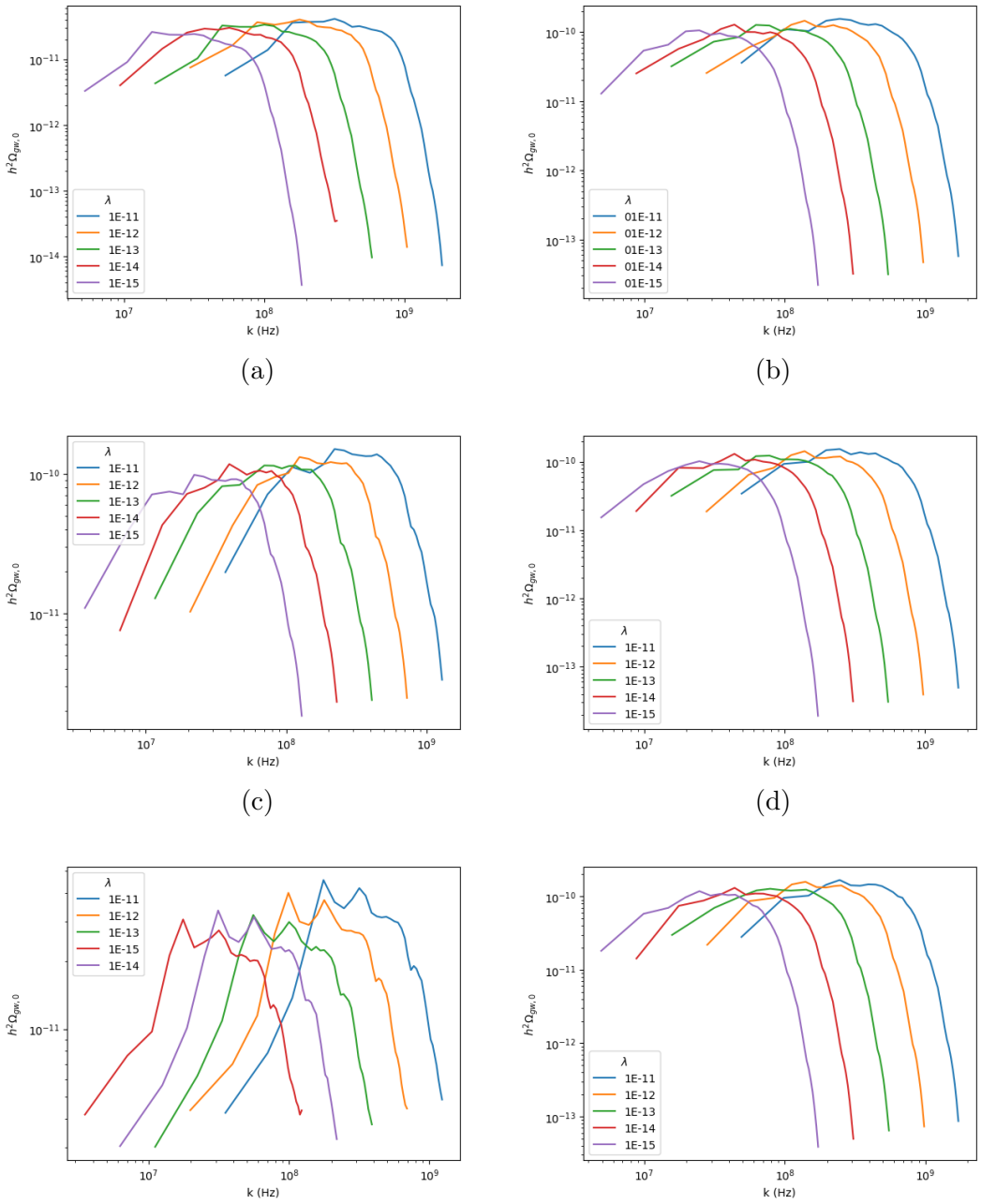

Figure 3.3: Gravitational wave signals in terms of frequency and amplitude. Each curve represents a signal with a different value of λ. Figures 3.3a - 3.3f correspond to signals from models 1 - 6.

We can similarly run a fit for each curve's λ, peak amplitude, and peak frequency. Results are shown in Table 3.1.

Model	$f^{peak}(\lambda)$ [s^{-1}]	$h^2\Omega^{peak}_{gw,0}(\lambda)$
1	$(1\times10^{11})\lambda^{1/4}$	$(2\times10^{-10})\lambda^{1/20}$
2	$(1\times10^{11})\lambda^{1/4}$	$(4\times10^{-10})\lambda^{1/25}$
3	$(1\times10^{11})\lambda^{1/4}$	$(4\times10^{-10})\lambda^{1/25}$
4	$(1\times10^{11})\lambda^{1/4}$	$(4\times10^{-10})\lambda^{1/25}$
5	$(5\times10^{10})\lambda^{1/5}$	$(1\times10^{-10})\lambda^{1/26}$
6	$(1\times10^{11})\lambda^{1/4}$	$(4\times10^{-10})\lambda^{1/25}$

Table 3.1: Table of relationships between λ and peak amplitude and frequency for different chaotic inflation models.

There are some generalities that we can take away from Fig 3.3 and Table 3.1. We can see that a signal's peak frequency is going to be much more sensitive to λ when compared to peak amplitude. Additionally, the relationships between λ and the peak quantities are very similar and the amplitudes and frequencies are all well within an order of magnitude within each other across models.

While the results are similar across models, the power law relations are not identical for all. We can see that Models 2 - 4, and 6 produce the same relationships, while Model 1 and Model 5 are different. In particular, Model 5 produces a peak frequency that is proportional to $\lambda^{1/5}$, which is different from the $\lambda^{1/4}$ proportionality that the other models produce.

We also want to look at λ's effect on β. Recall that this is the parameter from Giblin and Thrane's work defined in Eqn (2.11). This β parameter tells us 'how much source energy contributes to gravitational wave production.' To investigate β numerically, we define

$$\Gamma \equiv \frac{\Omega^{TT}_{gw,0}}{\Omega^{ALL}_{gw,0}}(k) \tag{3.3}$$

where

$$\beta = \frac{|T^{TT}_{ij}|^2}{|T_{ij}|^2} = \int \Gamma(k)dk. \tag{3.4}$$

Here, $\Omega^{TT}_{gw,0}$ is the gravitational wave energy density where HLattice strips out all but the transverse traceless components of the source's stress energy tensor. $\Omega^{ALL}_{gw,0}$ is the

simulated gravitational wave energy density having kept all components of the source's stress energy tensor. In comparing the two energy densities, we can learn about how much of the source's stress energy tensor is transverse-traceless, which is what β tells us.

The energy density $\Omega_{gw,0}^{ALL}$ is not a physical quantity. Only the transverse traceless components of the stress energy tensor contribute to actual gravitational wave production, but $\Omega_{gw,0}^{ALL}$ is a convenient quantity that we can compute from HLattice to tell us about β.

To graphically investigate β, we can use HLattice to give us gravitational wave energy density for both the TT case and the ALL case, use those spectra to compute Γ, and interpret the area under the Γ curve as β. Each Γ curve is going to have a different value of λ associated with it. With multiple Γ curves, we can then compare how β or the area under the Γ curves changes with λ while fixing $g^2/\lambda = 120$.

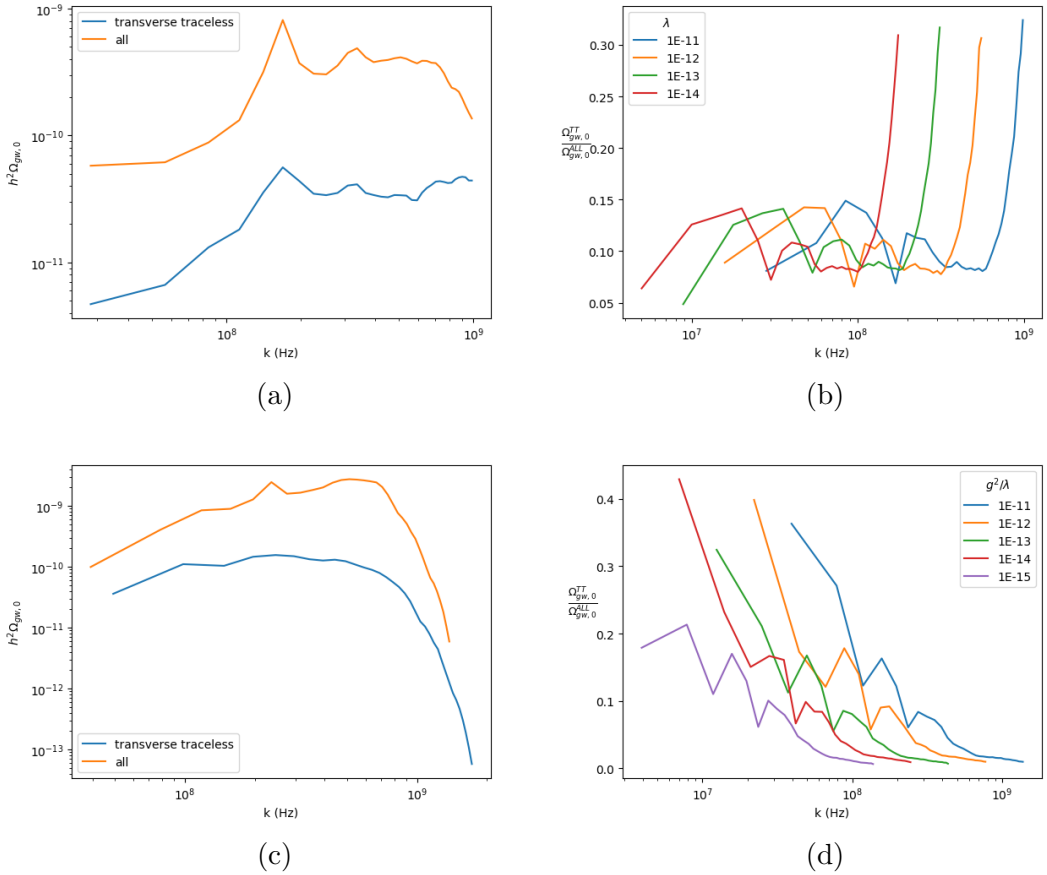

Figure 3.4: Fig. 3.4a shows the 2 different gravitational wave signals for $\lambda = 1 \times 10^{-11}$ where the curve labelled as 'all' is the spectrum where all components of the source's stress energy tensor are kept in the numerical simulation and the curve labelled as 'transverse traceless' is the spectrum where only the transverse traceless components of the source's stress energy tensor are kept. Each curve on Fig. 3.4b represents $\Omega^{TT}_{gw,0}$ divided by $\Omega^{all}_{gw,0}$ over k for a different value of λ. Fig. 3.4c and Fig. 3.4d are analogous to the plots in the first row, but the quantities are for Model 2 instead.

By inspecting Fig. 3.4, we see that the area under each Γ curve does not change much from curve to curve. This means that β does not change significantly from one value of λ to another. We saw in Fig. 3.1 that λ has a weak effect on amplitude. We can see that λ similarly has a weak effect on β.

Secondly, we expect to see changing λ produce a shift in frequency the same way changing λ produced a shift in frequency in Fig. 3.3. So it is reassuring to see that same shift in frequency in Fig. 3.3.

3.2 Results for g^2/λ

In this section, we will use HLattice to explore how gravitational wave frequency and amplitude change when we change our coupling parameter g^2/λ and hold λ fixed. We will, again, start with a Model 1 potential. Here we fix $\lambda = 10^{-14}$, which is the value needed to match CMB observations. The results are shown in Fig. 3.5.

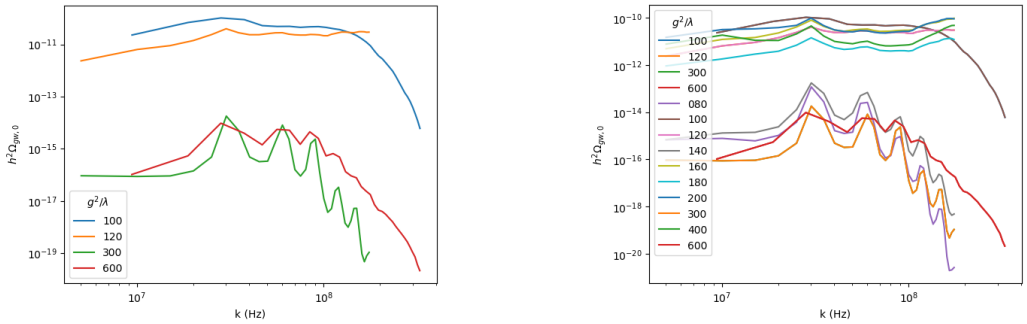

(a) (b)

Figure 3.5: Gravitational wave signals in terms of frequency and amplitude for different values of g^2/λ given a model 1 potential. Each curve represents a gravitational wave signal computed with a different value of g^2/λ. Fig 3.5a shows that 2 classes of high and low amplitude emerge as we let g^2/λ vary. Fig 3.5b shows that same bifurcation of amplitudes with more tested g^2/λ values.

The first and most obvious result is that g^2/λ has no effect on peak frequency. Each curve represents a gravitational wave with a different coupling parameter value and each curve sits on the same frequencies.

Second, there appear to be two distinct classes of amplitudes preferred for different couple parameter values: one class where $h^2\Omega_{gw,0}^{\text{peak}} \approx 10^{-10}$ and one class where $h^2\Omega_{gw,0}^{\text{peak}} \approx 10^{-15}$. There is not an obvious positive or negative relationship between amplitude and the chosen value of g^2/λ. We can see from Fig. 3.5a that $g^2/\lambda = 80$ falls in the lower amplitude class, $g^2/\lambda = 100, 120$ both fall in the higher amplitude class, and then $g^2/\lambda = 140$ falls back into the lower amplitude class.

We see that peak frequency is independent of or weakly dependent on g^2/λ, which is a clean conclusion to draw. But, the two distinct amplitude classes suggests a hairier

relationship between g^2/λ and amplitude. We are going to have to spend more time and thought investigating g^2/λ's effect on gravitational wave amplitudes.

We can try to track parameter values and peak amplitudes against different values of g^2/λ. We do this in Fig. 3.6.

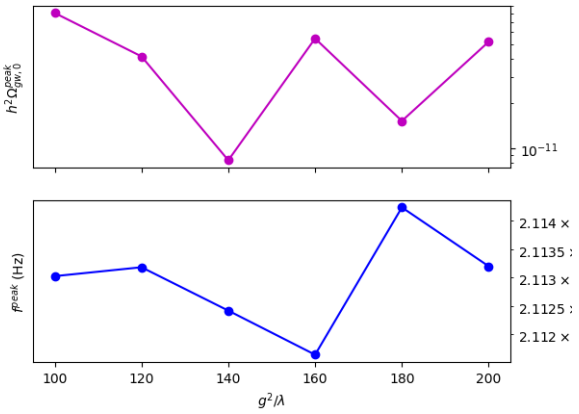

Figure 3.6: Each curve on Fig. 3.5 has a peak frequency, amplitude, and associated value of g^2/λ. Fig 3.2 tracks and plots the peak quantities with their associated values of g^2/λ.

Unlike in Fig. 3.2, Fig 3.6 does not show any simple relations like the ones in Table 3.1 that we can get between our parameter of interest g^2/λ and peak amplitude. We can infer from Fig. 3.2 and Fig. 3.6 that peak frequency depends very weakly on g^2/λ. This unclear relationship between g^2/λ and peak amplitude shown in Fig. 3.6 motivates us to dig deeper into the relationship between g^2/λ and amplitude. This analytic investigation is detailed in Chapter 5.

We can similarly simulate gravitational waves for different values of g^2/λ for other models. For each model, we then fit for peak gravitational wave amplitude, peak gravitational wave frequency, and g^2/λ as we did with Model 1. Simulated gravitational waves are shown in Fig. 3.7.

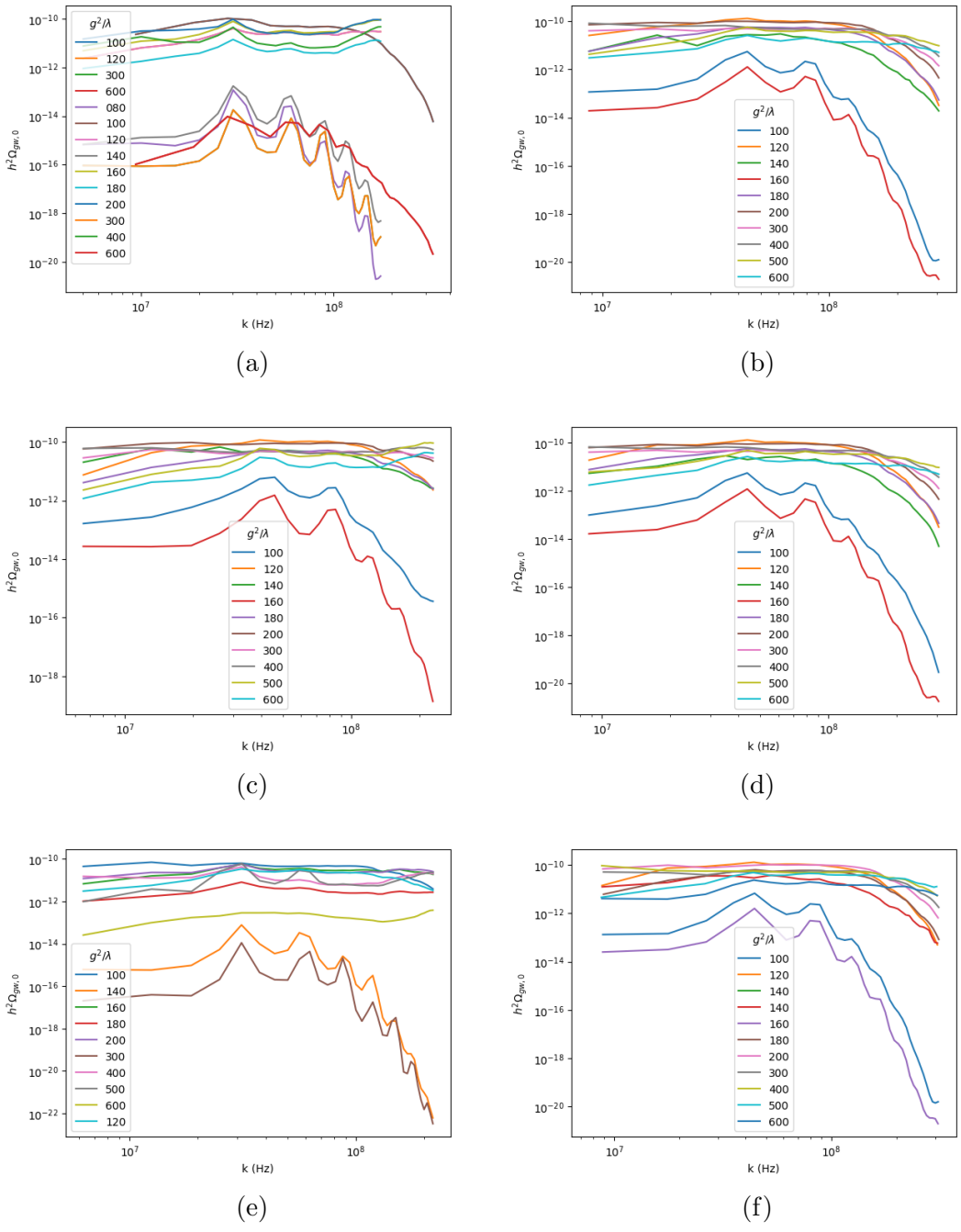

Figure 3.7: Gravitational wave signals in terms of frequency and amplitude for different g^2/λs given different potentials. Each curve represents a gravitational wave signal for a different value of g^2/λ. Figures 3.7a - 3.7f correspond to signals from models 1 - 6.

Some of our takeaways from examining model 1 still stand across models. For one, peak frequency appears to be independent of or weakly dependent on g^2/λ across models.

Furthermore, the relationship between g^2/λ and peak amplitude is still unresolvable with a simple curve fit.

We can also see the two-class amplitude behavior is also a feature across models. We also see that models 2, 3, 4, and 6 produce the same gravitational waves for the same coupling parameter values g^2/λ, while models 1 and 5 produce different waves for those same g^2/λ values.

It is worth investigating how β varies with g^2/λ to see what insight it can give us on this particular two-class amplitude puzzle. We can start by investigating how β and g^2/λ are related for a Model 1 potential.

Each Γ curve that we plot has a different value of g^2/λ associated with it. The area underneath each Γ curve is going to represent β for the value of g^2/λ associated with that curve. Results are shown in Fig 3.8.

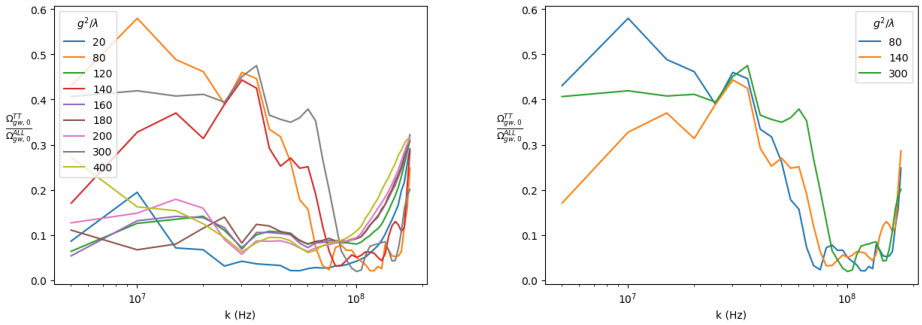

(a) (b)

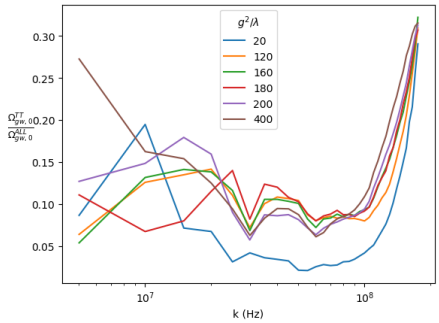

(c)

Figure 3.8: Each curve in Fig. 3.8a represents the fraction $\Omega^{TT}_{gw,0}$ divided by $\Omega^{all}_{gw,0}$ against k for a different value of g^2/λ. The curves on Fig. 3.8b and Fig. 3.8c are the same curves pulled from Fig. 3.8a. Fig. 3.8b shows curves where the area under each of them is higher (implying a higher β) than the area under each curve shown in Fig. 3.8c.

We set out to learn more about the two-class amplitude puzzle through β. We find two classes of β emerge from Fig. 3.8. Fig. 3.8b shows curves where chosen values of g^2/λ give high values of β. Fig. 3.8c shows curves where chosen values of g^2/λ give low values of β.

In Fig. 3.5, we saw higher amplitude gravitational wave signals for g^2/λ values of 80, 140, and 300. We also saw lower amplitude gravitational wave signals for g^2/λ values of 120, 160, 180, and 200. Fig. 3.8 shows that the same g^2/λ values that gave us low amplitude signals give us high values of β. The same g^2/λ values that gave us high amplitude signals give us low values of β.

This high amplitude-low β and low amplitude-high β result is not what we ex-

pected. A higher β signal would mean more of the source's stress energy tensor contributes to gravitational wave production. Therefore, our naive expectation suggests a higher β signal to correspond to the higher amplitude signals from Fig. 3.5a and the lower β signal to correspond to the lower amplitude signals. This is not what we find. Instead, we find the opposite.

We can also look at how β varies with g^2/λ for a Model 2 potential.

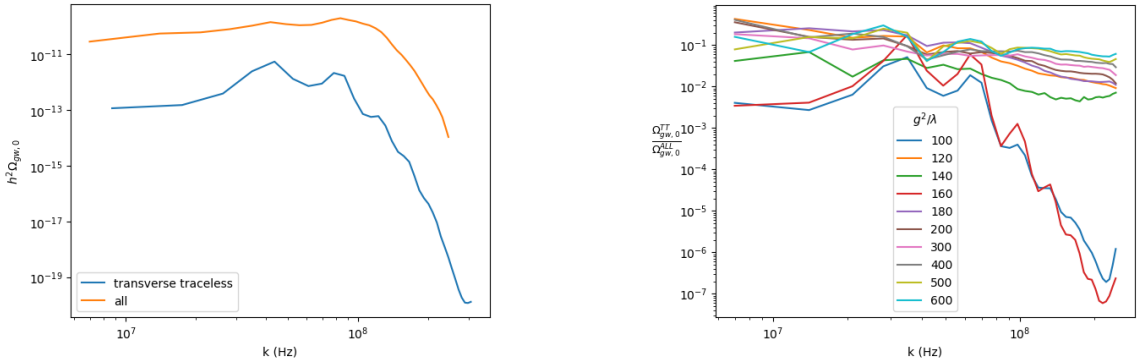

(a) (b)

Figure 3.9: Fig. 3.9a shows the 2 different gravitational wave signals for $g^2/\lambda = 120$ where the curve labelled as 'all' is the spectrum where all components of the source's stress energy tensor are kept in the numerical simulation and the curve labelled as 'transverse traceless' is the spectrum where only the transverse traceless components of the source's stress energy tensor are kept. Each curve on Fig. 3.9b represents $\Omega^{TT}_{gw,0}$ divided by $\Omega^{all}_{gw,0}$ over k for a different value of g^2/λ.

We can look at Fig. 3.9 and see that a high β and low β class emerge. Although for Model 2, the low β class has g^2/λ values associated with low amplitude signals and the high β class has g^2/λ values associated with high amplitude signals.

Chapter 4

A first order relation between λ and frequency

For most chaotic inflation models, Table 3.1 shows the peak frequency to be proportional to $\lambda^{1/4}$. We want to understand the what underlying physics would predict this.

Recall that ϕ and χ behave as coupled oscillators, where ϕ acts as the driving force, since $\phi \gg \chi$. This means that χ will respond to ϕ's driving frequency by amplifying certain modes. Therefore, χ's energy is unevenly distributed. This uneven distribution of energy gets produced at the driving frequency, giving us gravitational waves at the driving frequency.

If we wanted a more rigorous relationship for gravitational wave frequency, we would have to account for the perturbations in ϕ rather than just assuming that it is homogeneous all the way through the inflation and reheating process. But to first order, the gravitational wave frequency will match inflaton frequency. Therefore, we can estimate the gravitational wave frequency by computing the inflaton's frequency. A good starting point is the inflaton's equation of motion.

4.1 Frequency of the driving force

Assuming a homogeneous ϕ, ϕ obeys Eqn (1.15). This assumption should get us close enough to our earlier result Eqn (3.1). We also do not expect the small perturbations in ϕ to muddy up the $f^{peak} \propto \lambda^{1/4}$ relationship. This is because a system should oscillate at the frequency it is being driven at, and the driving frequency is determined by the homogeneous component of ϕ.

Because reheating occurs over a very small amount of time on Hubble scales, we are going to assume that the friction term is negligible, leaving us with $\ddot{\phi} + \frac{dV}{d\phi} = 0$. Next, we can assume our potential Eqn (2.22) to show that the inflaton's equation of motion homogeneous equation of motion becomes

$$\ddot{\phi} + \lambda\phi^3 + g^2\chi^2\phi = 0. \tag{4.1}$$

Now we can show why it was worth going about our numerical investigation of gravitational wave frequency's relation to λ and g^2/λ. Recall from Fig 3.5a that the coupling parameter g^2/λ has almost no effect on frequency. We saw this weak relation between g^2/λ and gravitational wave frequency because χ is going to be relatively small compared to ϕ. We can now simplify Eqn. 4.1 even further to

$$\ddot{\phi} + \lambda\phi^3 = 0. \tag{4.2}$$

This equation of motion is in dimensionless units (i.e, $\hbar = c = G = 1$). If we ultimately want our final result for λ and frequency to have any physical meaning, it will be important to express the final result where $\hbar, c, G$ are in units that have physical value. Recall from our analysis in Section 2.1.2 that we can get dimensionful quantities out by multiplying each factor of ϕ by $c/\hbar^{1/2}$ and λ by $1/\hbar$. A similar analysis shows that multiplying $\ddot{\phi}$ by $1/c^2$ will give us back dimensionful quantities.

4.1.1 Rescaling time units

Now we are going to rewrite our simplified equation of motion in terms of the units that we have been looking for. So our new physically meaningful equation of motion becomes

$$\frac{1}{c\hbar^{1/2}}\ddot{\phi} + \frac{\lambda c^3}{\hbar^{5/2}}\phi^3 = 0 \tag{4.3}$$

or

$$\frac{\hbar^2}{c^4\lambda}\frac{d}{dt}\frac{d}{dt}\phi + \phi^3 = 0.$$

where M_p is Planck mass. Recall from Eqn. (2.34) that we defined

$$\psi \equiv \frac{\phi}{\phi_0} \tag{4.4}$$

This allows us to again rewrite the equation as

$$\frac{1}{\phi_0^2}\frac{\hbar^2}{c^4\lambda}\frac{d}{dt}\frac{d}{dt}\psi + \psi^3 = 0.$$

Next, we can redefine our time unit to be

$$\tau \equiv \frac{c^2\phi_0\lambda^{1/2}}{\hbar}t. \tag{4.5}$$

where a unit of τ time corresponds to about 1.54×10^{-37} seconds assuming $\phi_0 = 3.5 \times M_p$. With this redefinition, we get

$$\frac{d^2\psi}{d\tau^2} + \psi^3 = 0 \tag{4.6}$$

This particular form of the equation of motion is useful because it is very easy to numerically evaluate for ψ's period and therefore its frequency.

4.1.2 Frequency at the end of inflation

We can see that Eqn. (4.5) gives us

$$f_j = \frac{c^2 \phi_0 \lambda^{1/2}}{\hbar} \frac{1}{\tau} \tag{4.7}$$

where f_j is the frequency at the end of inflation. The only thing we need to calculate f_j is the period. We numerically solve Eqn. (4.6) and find the period to be about 7.407 in units of τ. This period value gives us

$$f_j = (8.92 * 10^{42}\ \mathrm{s}^{-1})\ \lambda^{1/2}. \tag{4.8}$$

4.2 Accounting for redshift

While the relation between λ and gravitational wave frequency at the end of inflation f_j is interesting, we are not going to be observing gravitational wave signals at the end of inflation. We will be observing signals much later in time. Therefore, we need to also account for redshifted signals. And that means we will be measuring frequencies different from f_j.

To account for redshift, we will start by deriving a relation between scale factors and energy densities between today, the end of inflation, and thermal equilibrium [14]. We will denote quantities today, at the end of inflation, and at thermal equilibrium as q_o, q_j, and q_* respectively. We can start with

$$\frac{a_o}{a_j} = \frac{a_*}{a_j} \frac{a_o}{a_*}. \tag{4.9}$$

But, if we assume an entropy-conserving expansion, we can also say that

$$\frac{a_o}{a_*} = \frac{g_*^{1/3}}{g_o^{1/3}} \frac{T_*}{T_o}. \tag{4.10}$$

where g represents the degrees of freedom. Additionally, we can relate these temperatures to energy densities with

$$\rho_{relativistic} \propto gT^4 \tag{4.11}$$

giving us

$$\frac{a_o}{a_*} = \frac{g_*^{1/12}}{g_o^{1/12}} \frac{\rho_*^{1/4}}{\rho_o^{1/4}} \tag{4.12}$$

Now we can look at our starting Eqn (4.9) and see that we still need a_*/a_j

$$\frac{a_*}{a_j} = \rho_j^{1/4} \frac{\rho_*^{1/4}}{\rho_j^{1/4}} \rho_*^{-1/4} \frac{a^*}{a_j}. \tag{4.13}$$

We can recall our earlier solution to the equation relating density and scale factor Eqn (1.11) to get

$$\rho_* = \rho_j \left(\frac{a_*}{a_j} \right)^{-3(1+w)} \tag{4.14}$$

which we can combine with Eqn (4.9) and Eqn (4.12) to show

$$\frac{a_o}{a_j} = \left(\frac{\rho_j}{\rho_o} \right)^{1/4} \left(\frac{a_*}{a_j} \right)^{\frac{1-3w}{4}} \left(\frac{g_*}{g_o} \right)^{1/12}. \tag{4.15}$$

We can make some assumptions to simplify Eqn (4.15). We are going to assume that $w = 1/3$, implying a radiation dominated early universe. We also expect g_*/g_o to be around 100 in the Standard Model. Note that our choice for g_*/g_o is not too significant given the 1/12 power relationship between redshift and g_*/g_o.

Next, it is useful to see that a_o/a_j can be rewritten as Λ_o/Λ_j where Λ is wavelength, which can be rewritten again as f_j/f_o, where f is frequency. Knowing this and accounting for our simplifications, our relationship between frequency today and energy density can be simplified to

$$\frac{f_j}{f_o} = 100^{1/12} \left(\frac{H_j}{H_o} \right)^2. \tag{4.16}$$

So, the gravitational wave frequency f_o that we will measure today ought to be

$$f_o = \left(\frac{H_o}{100^{1/6} H_j}\right)^{1/2} f_j \tag{4.17}$$

This is useful to us because we can now compute f_o if we have the quantities f_j, H_o, and H_j. We have already calculated f_j Eqn (4.8). And while there is a healthy debate around the particular value of H_o, we are likely safe in assuming it to be approximately 70 km/s/Mpc. We also need a quantity H_j, or the Hubble parameter at the end of inflation. From the slow-roll parameter Eqn (1.23), we know that inflation ends when

$$\epsilon(\phi_j) = 1 = \frac{M_p^2}{2}\left(\frac{V'}{V}\right) \tag{4.18}$$

For a model 1 potential, we can compute ϕ_j to be $\phi_j \approx \sqrt{8} M_p$. We can now use the Friedmann Equation to compute the Hubble parameter H_j for a given field value ϕ_j. And because inflation ends when the kinetic term and potential term are approximately equal, we can make the following approximation:

$$H_j^2 = \frac{1}{3}\left(\frac{1}{2}\dot{\phi}^2 + V(\phi_j)\right) = \frac{2}{3} V(\phi_j). \tag{4.19}$$

Given a model 1 potential, we can estimate H_j to be approximately

$$H_j \approx (1.2 \times 10^{44}\ \mathrm{s}^{-1})\ \lambda^{1/2}. \tag{4.20}$$

Now we have everything we need to use Eqn (4.17) and find $f_o(\lambda)$.

$$\boxed{f_o \approx (8 \times 10^{11}\ \mathrm{s}^{-1})\ \lambda^{1/4}.} \tag{4.21}$$

We can compare this result to Eqn (3.1) and see that we recover the $f_o \propto \lambda^{1/4}$ behavior and the numerical factor in front is within an order of magnitude.

Chapter 5

An investigation of the quadrupolar parameter β

We were able to find a quick curve-fit relation between peak frequency and λ numerically. We were able to reproduce that numerical result analytically by integrating the driving force's equation of motion and redshifting the signal. In doing so, we can use future peak frequency observations to tell us about what λ value the underlying phenomenon ought to have.

We want to do something similar for gravitational wave amplitude. We found the effects of λ on amplitude to be quite muted in Table 3.1. On the other hand, Fig. 3.7 showed the effects of the coupling parameter g^2/λ on amplitude to be dramatic.

Recall from Eqn (2.11) that Giblin and Thrane were able to find a relationship between gravitational wave amplitude and the quadrupolar parameter β. They also mention how 'β is the hardest parameter to estimate without specific knowledge of the source.' Conversely, this suggests that given specific knowledge of the source, we can learn a great deal about how the source and signal are connected to each other. So in this chapter, we will use reheating after chaotic inflation as a specific cosmological source of gravitational waves. Then we will see how β depends on inflation parameters.

Giblin and Thrane made two major assumptions about the source's stress energy tensor: it is Gaussian distributed in k-space about some characteristic k_* and it has a random complex phase factor associated with each component. From there, they numerically estimate β by randomly generating complex phase factors and assume each component to be approximately equal in magnitude.

We do not have to start with those assumptions. β is defined as a ratio between the transverse traceless projection of the source's stress energy tensor and the source's stress energy tensor itself. So without assuming a complex phase factor or a Gaussian distribution, we can write the stress energy tensor of some scalar field χ as

$$\tilde{T}_{ij}(\mathbf{k}) = (\partial_i \chi)(\partial_j \chi)(\mathbf{k}). \tag{5.1}$$

We are going to use the following Fourier transform convention

$$\begin{aligned} f(\mathbf{x}) &= \int \frac{d^3\mathbf{k}}{(2\pi)^{3/2}} f(\mathbf{k}) e^{-i\mathbf{k}\cdot\mathbf{x}} \\ \tilde{f}(\mathbf{k}) &= \int \frac{d^3\mathbf{x}}{(2\pi)^{3/2}} f(\mathbf{x}) e^{i\mathbf{k}\cdot\mathbf{x}} \end{aligned} \tag{5.2}$$

and assume the following wave packet form for $\chi(\mathbf{x})$:

$$\chi(\mathbf{x}) = \int \frac{d^3\mathbf{p}}{(2\pi)^{3/2}} f(\mathbf{p}) e^{-i\mathbf{p}\cdot\mathbf{x}}. \tag{5.3}$$

This means that

$$\partial_i \chi(\mathbf{x}) = -i \int \frac{p_i d^3\mathbf{p}}{(2\pi)^{3/2}} f(\mathbf{p}) e^{-ip_i x_i} \tag{5.4}$$

where $\mathbf{p}$ is the dummy momentum variable and $f(\mathbf{p})$ is the functional form for our field amplitude in p-space. Given this form of $\partial_i \chi(\mathbf{x})$, we can represent the stress energy

tensor in position-space as

$$T_{ij}(\mathbf{x}) = (\partial_i \chi(\mathbf{x}))\,(\partial_j \chi(\mathbf{x})) = \int \frac{p_i' d^3\mathbf{p}'}{(2\pi)^{3/2}} f(p_i') e^{-ip_i' x_i} \int \frac{p_j d^3\mathbf{p}}{(2\pi)^{3/2}} f(p_j) e^{-ip_j x_j}. \tag{5.5}$$

We can then take the Fourier transform of $T_{ij}(\mathbf{x})$ and find

$$\tilde{T}_{ij}(\mathbf{k}) = \frac{1}{(2\pi)^{3/2}} \int p_i (p_j - k_j) f(\mathbf{p}) f(\mathbf{k} - \mathbf{p}) d^3\mathbf{p}. \tag{5.6}$$

We need some functional form for our field amplitude f. Here is where we apply specific information about chaotic inflation to find $T_{ij}(\mathbf{k})$.

Recall that the field responsible for sourcing reheating is χ. We can rely on the rescaled equation of motion Eqn (2.28) for X_k (where $X_k = a\chi$ for a particular k) that Dufaux et al use to learn about what functional form is appropriate for χ. To compute X_k from its equation of motion, we need to compute the frequency term ω_k in Eqn (2.29). ω_k is going to depend on ϕ. We can compute ϕ from its homogeneous one-dimension equation of motion Eqn (1.15). ϕ depends on our choice for $V(\phi)$.

Now we numerically integrate ϕ for our different potentials $V(\phi)$ discussed earlier in Eqn (2.34), combine those results for ϕ into Eqn (2.28) to compute X_k and see what generalities and observations we can learn about χ and its amplitude given different inflaton potentials $V(\phi)$. The results for X_k over x (or $\sqrt{\lambda}\phi_0 t$) for different inflaton potentials $V(\phi)$ is shown in Fig. 5.1.

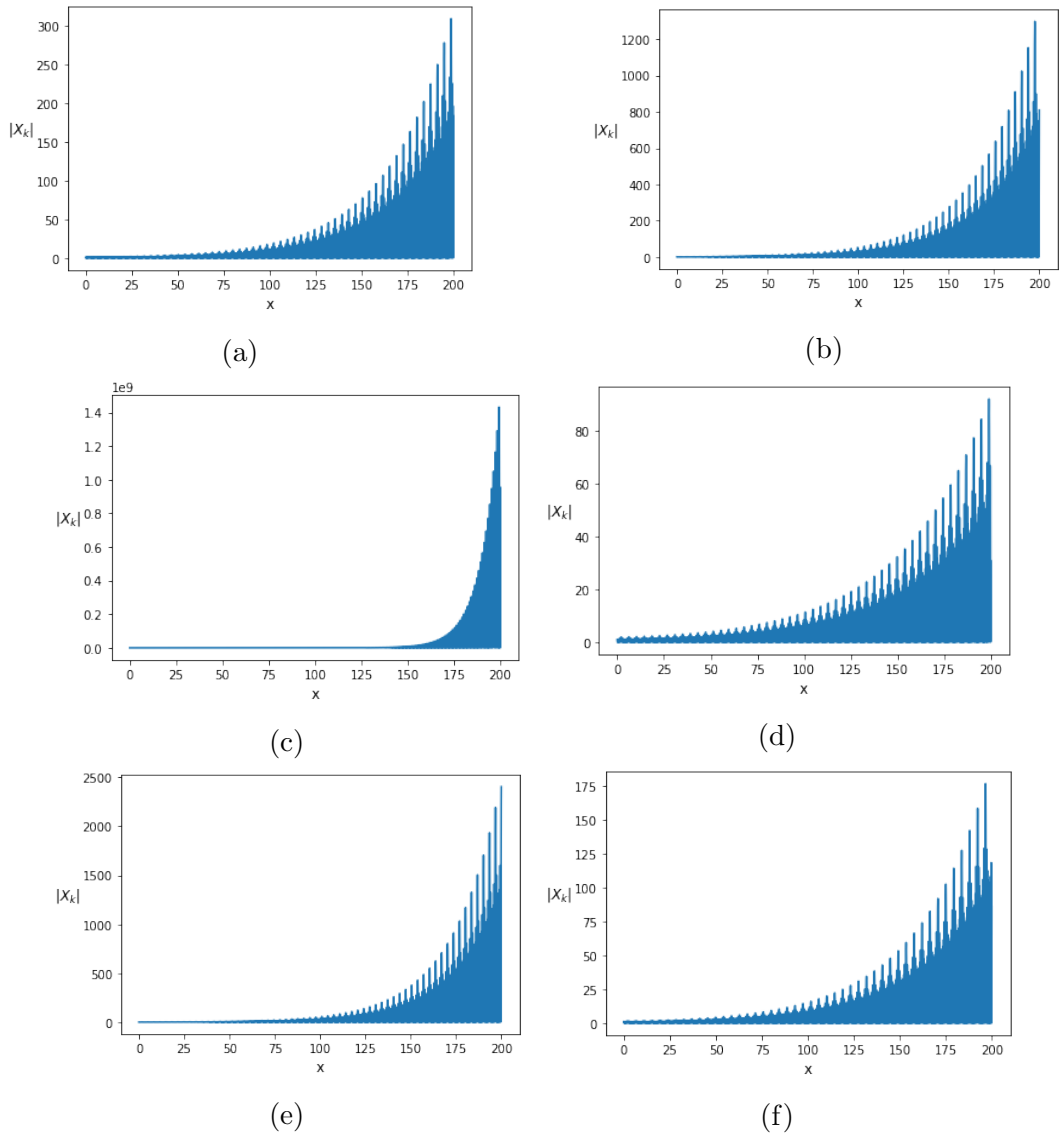

Figure 5.1: $|X_k|$ against rescaled time x for $V(\phi)$ models 1 - 6 for Fig. 5.1a - 5.1f respectively. These all correspond with different coupling parameter values g^2/λ or q.

For each potential, we see that, for certain coupling parameters q or g^2/λ, we get parametric resonance. This exponential growth in χ can be described by some

$$|\chi|(x) = Ae^{\mu x} \tag{5.7}$$

where μ is the parameter describing the rate of exponential growth in amplitude against our rescaled time x and A is the initial amplitude. We investigated how this exponential

growth parameter μ changed for different coupling parameters q or g^2/λ and for different models. In investigating the exponential growth rate's sensitivity to g^2/λ or q, we found that μ is very weakly if at all dependent on q. We found that across models, μ is on the order of 10^{-2}.

We have computed some form of χ, but Eqn. (5.6) requires our functional form for our field's amplitude to be in momentum space. We can compute what $\chi(k)$ ought to look like by choosing some q for each potential model, letting k vary in Eqn (2.29), and computing $|X_k|$ for different k values while holding q and x fixed. What we get can be shown in Fig. 5.2.

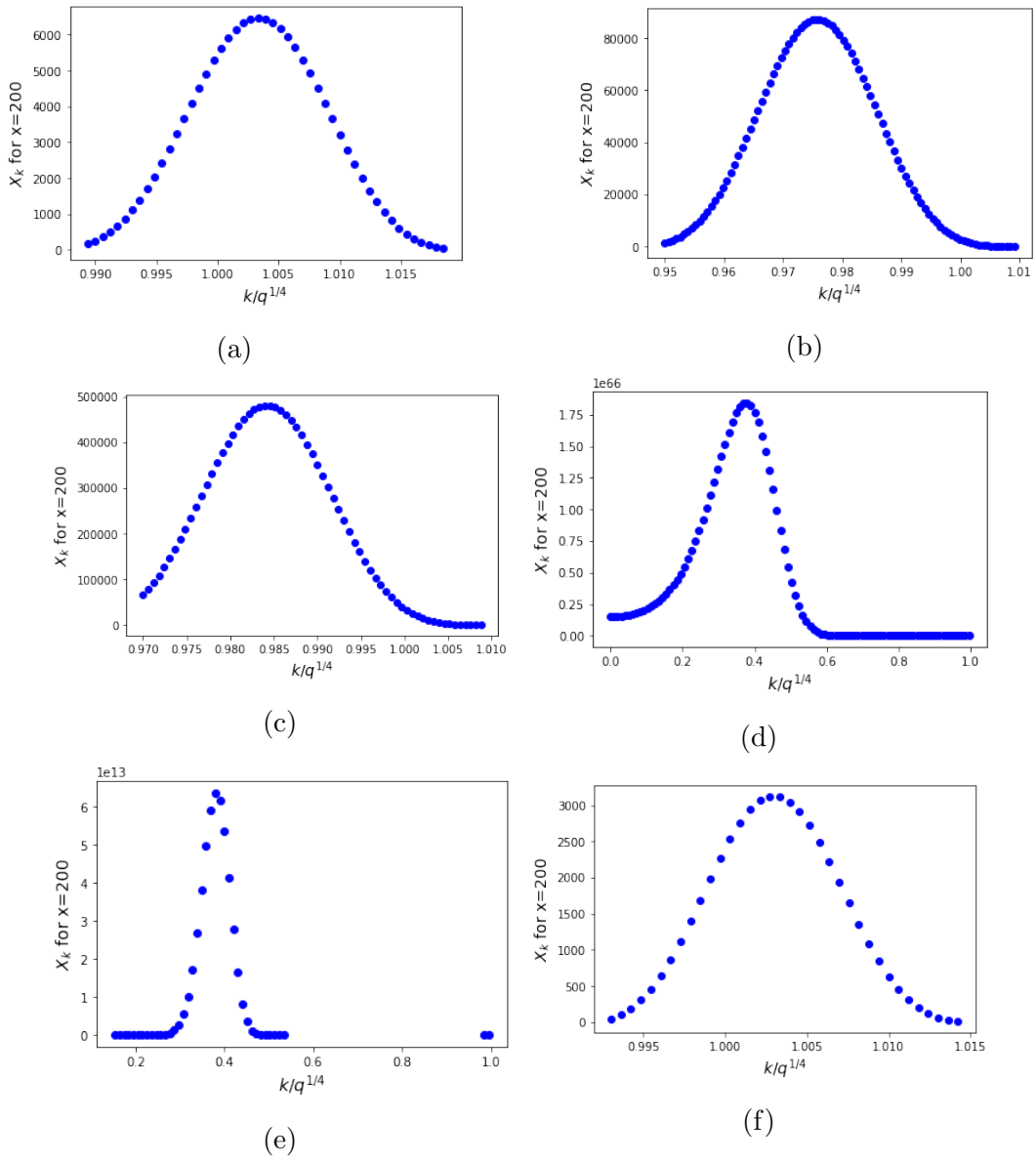

Figure 5.2: $|X_k|$ against k expressed as a ratio of $q^{1/4}$ for $x = 200$ for $V(\phi)$ models 1 - 6 for Fig. 5.2a - 5.2f respectively.

Recall we were trying to compute $T_{ij}(\mathbf{k})$ and needed a functional form for our scalar field $f(\mathbf{p})$ in Eqn (5.6). We can see that $f(\mathbf{p})$ can take on a Gaussian form which can be written as

$$f(\mathbf{p}) = \chi_0 e^{-\alpha(\mathbf{p}-\mathbf{k}_*)^2} \tag{5.8}$$

where χ_0 is some characteristic amplitude, α characterizes the standard deviation, and

k_* is the characteristic momentum roughly distributed about $(g^2/\lambda)^{1/4}$. We are going to assume an isotropic source term, meaning we do not expect any differences in f in any one particular direction or another

$$f(\mathbf{p}) = \chi_0 e^{-\alpha(p-k_*)^2}. \tag{5.9}$$

We then combine Eqn (5.9) with Eqn (5.6) to get

$$T_{ij}(k) = \frac{\chi_0^2}{(2\pi)^{3/2}} \int p_i(p_j - k_j) f(p) f(k-p) p^2 dp \sin\theta d\theta d\varphi \tag{5.10}$$

which evaluates to

$$T_{ij}(k) = -\chi_0^2 \frac{96(\alpha^2 k^4 - 3)}{\alpha^{5/2}} e^{-\frac{\alpha}{2}(k-2k_*)^2}. \tag{5.11}$$

We can then compute

$$|T_{ij}|^2 = \frac{3\chi_0^4}{9216} \frac{(\alpha^2 k^4 - 3)^2}{\alpha^5} e^{-\alpha(k-2k_*)^2} \tag{5.12}$$

This puts us one step closer to computing β in terms of chaotic inflation parameters. We find all components of T_{ij} to be the same. This is reassuring. Because the source is isotropic, we shouldn't expect a stronger or weaker measurement in one direction versus another.

We hypothesize that the dependency between the source energy tensor and chaotic inflation parameters is going to be encoded in the characteristic momentum k_*, which is approximately $(g^2/\lambda)^{1/4}$. All that is left for computing β is to compute $T_{ij}^{TT}(\mathbf{k})$ by applying the transverse traceless projection operator $\mathcal{O}_{ij,\ell m}$ on $T_{ij}(\mathbf{k})$ as shown in Eqn (2.19).

$T(\mathbf{k})$ is going to be a function of vector $\mathbf{k}$. We are going to define $\mathbf{k}$ to be in the $\hat{\mathbf{z}}$ direction. We can do this because the source will be, on large scales, homogeneous, in all directions. So what direction we choose the source to be oriented in is arbitrary. With

this assumption, our projection operator becomes

$$P_{ij} = \delta_{ij} - \hat{k}_i \hat{k}_j = \begin{pmatrix} 1 & 0 & 0 \\ 0 & 1 & 0 \\ 0 & 0 & 0 \end{pmatrix}. \tag{5.13}$$

We can now combine Eqn (5.13) with Eqn (2.19) and get

$$T_{ij}^{TT} = \frac{\chi_0^2}{(2\pi)^{3/2}} \int \mathcal{O}_{ij,\ell m} p_\ell p_m e^{-\alpha(p-k_*)^2} e^{-\alpha(k-p-k_*)^2} d^3p \tag{5.14}$$

The following components fall out of when we evaluate this:

$$\begin{aligned} T_{xx}^{TT} &= \frac{\chi_0^2}{2(2\pi)^{3/2}} \int_0^\pi \sin^3\theta d\theta \int_0^{2\pi} (\cos^2\varphi - \sin^2\varphi) d\varphi \int p^4 e^{-\alpha(p-k_*)^2} e^{-\alpha(k-p-k_*)^2} dp \\ T_{yy}^{TT} &= -\frac{\chi_0^2}{2(2\pi)^{3/2}} \int_0^\pi \sin^3\theta d\theta \int_0^{2\pi} (\sin^2\varphi - \cos^2\varphi) d\varphi \int p^4 e^{-\alpha(p-k_*)^2} e^{-\alpha(k-p-k_*)^2} dp \\ T_{xy}^{TT} &= \frac{\chi_0^2}{2(2\pi)^{3/2}} \int_0^\pi \sin^3\theta d\theta \int_0^{2\pi} \cos\varphi \sin\varphi d\varphi \int p^4 e^{-\alpha(p-k_*)^2} e^{-\alpha(k-p-k_*)^2} dp \end{aligned} \tag{5.15}$$

where φ is the azimuthal angle and θ is the polar angle. The integral over the polar angle evaluates to $4/3$ in each case and the integral over p evalutes to

$$\frac{\sqrt{\frac{\pi}{2}}(3 + \alpha k^2(6 + \alpha k^2))}{32\alpha^{5/2}} e^{-\frac{\alpha}{2}(k-2k_*)^2}. \tag{5.16}$$

But we also find that the integral over the azimuthal angle evaluates to zero for all $f(p)$. In other words, T_{ij}^{TT} is zero for all components, meaning our quadrupolar parameter β and gravitational wave amplitude *vanish*.

We had originally set out to study gravitational wave production from reheating with the simplest starting point possible by assuming homogeneity and using ϕ's one-dimension equation of motion to compute ϕ and using that to compute χ and then the source. This ultimately gives us no gravitational wave spectrum. But, our calculation

shows what we ought to do next. We are getting no gravitational wave spectrum because our integral over the azimuthal angle vanishes. This is due to our assumption of source isotropy. We can reintroduce anisotropy through small perturbations in our initial conditions. Moving forward, we need to learn how initial anisotropies grow and how these anisostropies contribute to T_{ij}^{TT}.

However, one thing we can do with our current result is do an order-of-magnitude approximation of β. We know that the integral over small perturbations along the azimuthal angle is going to give us a result on the order of one. So if we assume the integral over the azimuthal angle to be one for each component of the T_{ij}^{TT}, we find

$$|T_{ij}^{TT}|^2 = \frac{\chi_0^4}{384\pi^3}\frac{(3+\alpha k^2(6+\alpha k^2))^2}{\alpha^5}e^{-\alpha(k-2k_*)^2}. \tag{5.17}$$

We want to compare our estimate of β with Giblin and Thrane's estimate. They take β to be the average of $|T_{ij}^{TT}|^2$ over the average of $|T_{ij}|^2$ over all k-space. So, we are going to integrate Eqn (5.17) over all k-space and divide by the integral of Eqn (5.11) over all k-space. In doing so, we find

$$\beta = \frac{1}{8\pi^2}\frac{140+32k_*^2(699+4k_*^2(369+16k_*^2(13+2k_*^2)))}{177+32k_*^2(69+372k_*^2+448k_*^4+128k_*^6)}. \tag{5.18}$$

Recall that $k_* \approx (g^2/\lambda)^{1/4}$. We let $g^2/\lambda = 120$ and $\alpha = 1$. This gives us

$$\beta \approx 0.016. \tag{5.19}$$

Recall that Giblin and Thrane estimated this β to between 10^{-2} and $10^{-1.5}$ or between. This estimate for β falls within that range. We also want to know how this parameter varies for different qs. β approaches 0.0127 as $q \to \infty$ and 0.01 as $q \to 0$. Thus, we get good agreement between our estimate and past estimates, implying we have captured a good piece of the core physics involved in gravitational wave production.

While this agreement is nice, it still does not explain the two-class amplitude puzzle we found in Fig 3.7. This β function is nice and continuous and nearby values of q give nearby values of β. Therefore, there is still important physics related to gravitational wave production that we have not captured in this estimate for βs.

Chapter 6

Discussion

6.1 The two-class amplitude puzzle

Fig. 3.7 showed that the two-class amplitude behavior appears across all potentials explored in this project. There are a few strategies we investigate this two-class amplitude puzzle further. We can compare the time evolution of a high-amplitude signal and a low-amplitude signal and see when along the process of reheating they diverge into their separate classes. Doing so can tell us which stage of reheating to focus our studies on. The results for this analysis can be shown in Fig. 6.1.

Fig. 6.1 shows that both signals start out close together, meaning that the signals do not start in their separate amplitude classes. Instead, the gravitational wave amplitudes grow further apart and separate into their respective amplitude classes over time or scale factor. Fig. 6.1b shows that this divergence happens at around a scale factor of $a = 20$ and the divergence slows at a scale factor of about $a = 60$.

However, the values of scale factor are not immediately meaningful. They only tell us how much larger this simulated Universe is relative to some chosen starting point. However, we can gain meaning from these scale factor values by looking at the evolution of peak amplitude against time (or scale factor) and seeing what kind of growth these

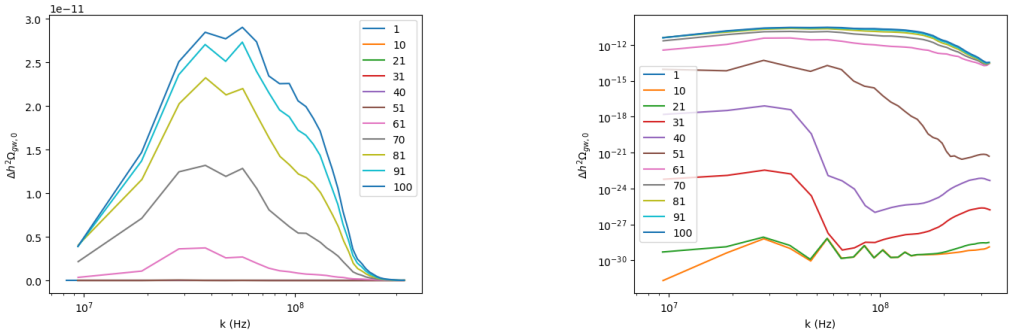

(a) (b)

Figure 6.1: $\Delta h^2\Omega_{gw,0}$ is the difference in $h^2\Omega_{gw,0}$s between the high amplitude signal and the low amplitude signal. Each curve represents that amplitude difference for a different scale factor a. Fig. 6.1a shows this for model 1 on a linear scale and Fig. 6.1b shows that same difference on a log scale.

scale factor values correspond to. Different growth behaviors correspond to different periods of reheating. The time evolution of peak amplitude can be shown in Fig. 6.2.

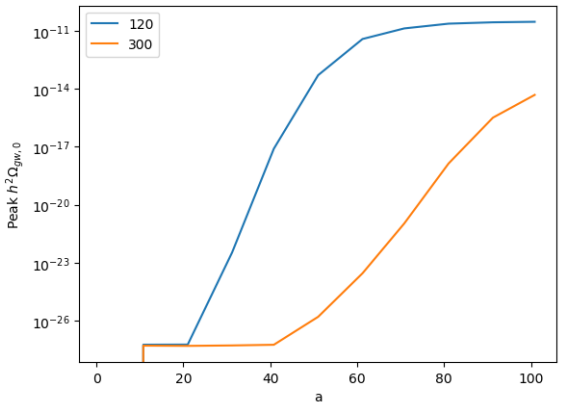

Figure 6.2: Evolution of two signals' peak amplitudes for $g^2/\lambda = 120$ and $g^2/\lambda = 300$ against time (scale factor) for a model 1 potential

There are a few points we can learn from Fig. 6.2. First, we can see that these two different class of gravitational waves have different exponential growth rates. So given a relationship of

$$\text{peak amplitude we might observe today} = |A|e^{\mu a} \tag{6.1}$$

the μ parameter or rate of exponential growth is higher for that of $g^2/\lambda = 120$ than

$g^2/\lambda = 300$.

Second, we can see that this divergence in high and low amplitude signals occur at the exponential growth stage of reheating. We can see this to be the case for a variety of g^2/λs in Fig. 6.3.

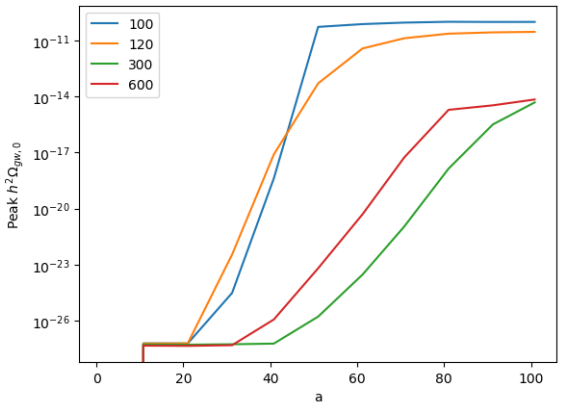

Figure 6.3: Evolution of two signals' peak amplitudes for more values of g^2/λ.

So if we want to learn more about the two-class amplitude puzzle, we want to focus our studies on gravitational wave production during the exponential growth phase of reheating.

6.2 β - An estimate for reheating

We concluded that, given a completely real Gaussian distributed χ amplitude, β vanishes. In other words, we get no gravitational waves. In hindsight, we should have expected this result. Dufaux et al have already predicted this result from what they call their 'no-go theorem,' which states that "scalar field configurations which can be represented as the superposition of waves with wave-like dispersion relations and adiabatically varying frequencies do not emit gravity waves at first order in the gravitational coupling."

This no-go theorem means that if our scalar field's frequency can be modelled as a simple sum of waves (which a Gaussian certain can be), we should not expect gravitational

waves. Dufaux et al make this prediction by making a conservation of helicity argument. The graviton (which acts as the particle analog to gravitational waves) has a helicity of 2 and the interacting scalar waves (in our case, ϕ and χ) have helicities 0. In any given interaction, helicity must be conserved. And two scalar waves of helicity 0 cannot produce a graviton of helicity 2 alone.

In our case, we make a direct calculation of this no-go theorem. We have a specific wave-like scalar field model and evaluate T_{ij}^{TT} to be zero given that model.

But, we ultimately do want to learn how we can recover gravitational waves. After all, the simulation is getting non-zero signals. There are a few options we can explore about our earlier assumptions.

We want our integral over φ or the azimuthal angle between $\mathbf{p}$ and $\mathbf{k}$ to be nonzero. So we need to find where we can get extra φ dependence in our integral over χ.

Our calculation of T_{ij}^{TT} assuming isotropy, meaning that χ has no directional dependence or preference. We made the same assumption of $\phi(\mathbf{k})$. We assumed this because the source's stress energy tensor is expected to be, on large scales, homogeneous and to have no directional preference. However, gravitational waves are only produced if there are ultimately inhomogeneities in energy distributions. Further investigation into how initial conditions play a role in ϕ and χ behavior could give us insight into any potential directional dependence that might emerge in T_{ij}^{TT}.

Additionally, we assumed that χ was all real in k-space. And that assumption led us to a vanishing β parameter. Recall from Eqn (2.1), Giblin and Thrane assumed the energy tensor to have a complex phase factor associated with it as well. What this complex phase factor is and how it might be modelled can also play a role in giving us non-vanishing β. For now, we can clearly see that assuming a purely real source gives us vanishing β.

While there is clearly more we can investigate about β, we were still able to do an approximate calculation of β by considering what would happen if the integral over

initial perturbations along the azimuthal angle were nonzero. The integral over random fluctuations would be on the order of one. With that approximation, we were able to compute β to relatively good agreement with previous estimates.

While the agreement means we are on the right track of capturing the relevant physics involved in β and gravitational wave production, our calculation for β did not give any insight into the two-class amplitude puzzle. So, we still need to find a way to account for that. A good starting point for that is reheating during the exponential growth stage, as we found in Fig 6.2.

6.3 Conclusion

We wanted to refine our understanding of cosmological gravitational wave production during reheating in order to improve our ability to interpret these signals on the day we actually get to see them.

In our numerical investigations, we found that the coupling parameter g^2/λ had no effect on frequency and that most chaotic inflation models had a peak frequency proportional to $\lambda^{1/4}$. We were able to find that same proportionality through our first order analytic investigation. We did this by approximating the gravitational wave signals to respond at the same frequency as its driving force (the inflaton oscillations), assuming that g^2/λ had no effect on frequency, and then redshifting the initial frequency relationship. This result is useful because it provides a direct relationship between an observable quantity and a model parameter.

In particular, different models will have different values of λ. Being able to look at a peak frequency and then identify a particular value for λ will enables us to identify what model properly describes inflation.

In our numerical investigations, we also found that the parameter with the dominant influence on amplitude was the coupling parameter g^2/λ. We also found two classes

of amplitudes for otherwise close values of the coupling parameter. While we are still unable to explain this result in its entirety, we found that these classes emerge during the exponential pre-heating phase after reheating. Knowing this will focus what stage of reheating we choose to study to learn more about gravitational wave production from reheating.

In our analytic investigation of the quadrupolar parameter β, we constructed a toy model that features the core scalar field physics involved with gravitational wave production from reheating. We built a model that calculated ϕ, which we could then use to calculate χ. We found that χ grew exponentially over time, and that χ's amplitude could be represented in k-space as a Gaussian about some mean frequency k_*.

We used this real Gaussian form for χ's amplitude to compute the source's stress energy tensor, applied the transverse traceless projection operator to the stress energy tensor, and found that the transverse traceless components of the stress energy tensor vanished, and β along with them. This process of computing ϕ, then χ, then the source is a direct sequence of calculations showing the no-go theorem, which states that interacting scalar fields that can be represented with a wave-like dispersion relation ought to give no gravitational waves.

In our calculation for β, we found that components of the source's stress energy tensor disappear because each component's integral over its azimuthal angle disappear. In order to recover gravitational waves in future studies, we re-introduce directional dependence by studying initial fluctuations in χ.

In the meantime, we did an order of magnitude estimate of β by assuming the integral over these initial random fluctuations to be on the order of one. In doing so, we estimated β to fall within 0.0100 and 0.0713, which agrees with estimates done by previous researchers.

In summary, we found an analytic first-order relation between cosmological gravitational wave frequency and inflation parameters. We have more investigation to do

with regards to the amplitude relationship. But our estimate of β suggests we are on the right track. We have strings that we can pull on to investigate β and the two-class amplitude puzzle further. In particular, we can think more carefully about how initial fluctuations can give us a non-zero β, and we know to think about gravitational wave amplitude in the context of the exponential preheating growth phase of reheating. While we have some more exploring left to do, we are not lost.

Acknowledgments

First, I want to thank Jeffrey Hyde for introducing me to and helping me navigate this project, for extracting me from frustrating spirals, for believing in me even when I did not, and for showing me that I am and can become more than I imagined.

I also want to thank the entire Bowdoin Physics faculty and staff for teaching me to be more patient, independent, empathetic, and confident; for putting up with my strange and superfluous antics in the classroom, in Searles, and over email.

I want to thank all my fellow physics classmates who braved the cold and stormy sea of problem sets alongside me, pulled me out of the water when I fell overboard, steered me in the right direction when I was lost, and whose company kept me warm.

I want to thank Chloe Richards and Maria Perez Mendoza for being that for me for four years. I wish you both well on the remainder of your respective voyages. It has been my privilege to sail alongside the two of you. Best of luck!

References

[1] Alan H. Guth. "The Inflationary Universe: A Possible Solution to the Horizon and Flatness Problems". In: *Phys. Rev. D* 23 (1981). Ed. by Li-Zhi Fang and R. Ruffini, pp. 347–356. DOI: 10.1103/PhysRevD.23.347.

[2] Andrei D. Linde. "A New Inflationary Universe Scenario: A Possible Solution of the Horizon, Flatness, Homogeneity, Isotropy and Primordial Monopole Problems". In: *Phys. Lett. B* 108 (1982). Ed. by Li-Zhi Fang and R. Ruffini, pp. 389–393. DOI: 10.1016/0370-2693(82)91219-9.

[3] Jean Francois Dufaux et al. "Theory and Numerics of Gravitational Waves from Preheating after Inflation". In: *Phys. Rev. D* 76 (2007), p. 123517. DOI: 10.1103/PhysRevD.76.123517. arXiv: 0707.0875 [astro-ph].

[4] John T. Giblin and Eric Thrane. "Estimates of maximum energy density of cosmological gravitational-wave backgrounds". In: *Phys. Rev. D* 90.10 (2014), p. 107502. DOI: 10.1103/PhysRevD.90.107502. arXiv: 1410.4779 [gr-qc].

[5] Dan Hooper et al. "Can the Inflaton Also Be a Weakly Interacting Massive Particle?" In: *Phys. Rev. Lett.* 122.9 (2019), p. 091802. DOI: 10.1103/PhysRevLett.122.091802. arXiv: 1807.03308 [hep-ph].

[6] Edwin Hubble. "A relation between distance and radial velocity among extragalactic nebulae". In: *Proc. Nat. Acad. Sci.* 15 (1929), pp. 168–173. DOI: 10.1073/pnas.15.3.168.

[7] M. C. Guzzetti et al. "Gravitational waves from inflation". In: *Riv. Nuovo Cim.* 39.9 (2016), pp. 399–495. DOI: 10.1393/ncr/i2016-10127-1. arXiv: 1605.01615 [astro-ph.CO].

[8] Katie Chamberlain and Nicolas Yunes. "Theoretical Physics Implications of Gravitational Wave Observation with Future Detectors". In: *Phys. Rev. D* 96.8 (2017), p. 084039. DOI: 10.1103/PhysRevD.96.084039. arXiv: 1704.08268 [gr-qc].

[9] K. Riles. "Gravitational Waves: Sources, Detectors and Searches". In: *Prog. Part. Nucl. Phys.* 68 (2013), pp. 1–54. DOI: 10.1016/j.ppnp.2012.08.001. arXiv: 1209.0667 [hep-ex].

[10] Seiji Kawamura et al. "Current status of space gravitational wave antenna DECIGO and B-DECIGO". In: (June 2020). arXiv: 2006.13545 [gr-qc].

[11] Richard Easther et al. “Gravitational Wave Production At The End Of Inflation”. In: *Phys. Rev. Lett.* 99 (2007), p. 221301. DOI: 10.1103/PhysRevLett.99.221301. arXiv: astro-ph/0612294.

[12] Zhiqi Huang. “The Art of Lattice and Gravity Waves from Preheating”. In: *Phys. Rev. D* 83 (2011), p. 123509. DOI: 10.1103/PhysRevD.83.123509. arXiv: 1102.0227 [astro-ph.CO].

[13] James M. Cline. “TASI Lectures on Early Universe Cosmology: Inflation, Baryogenesis and Dark Matter”. In: *PoS* TASI2018 (2019), p. 001. arXiv: 1807.08749 [hep-ph].

[14] Julian B. Muñoz and Marc Kamionkowski. “Equation-of-state parameter for reheating”. In: *Phys. Rev. D* 91 (4 Feb. 2015), p. 043521. DOI: 10.1103/PhysRevD.91.043521. URL: https://link.aps.org/doi/10.1103/PhysRevD.91.043521.